

UNIVERSITA' DEGLI STUDI DI PARMA

Dottorato di ricerca in Fisiopatologia Sistemica

Ciclo XXVI

***Isolation and characterization of a human cell line
from Non Small Cell Lung Cancer***

Isolamento e caratterizzazione di una linea cellulare umana
da Non Small Cell Lung Cancer

Coordinatore:
Chiar.mo Prof. Enrico Maria Silini

Tutor:
Chiar.mo Prof. Federico Quaini

Dottorando:
Dott.ssa Angela Falco

INDEX

INTRODUCTION

Pag.5

LUNG CANCER

EPIDEMIOLOGY

ETIOLOGY

HISTOLOGY

CLINICAL AND THERAPEUTIC ASPECTS

HUMAN STEM CELLS

HUMAN LUNG STEM CELLS

CANCER STEM CELL AND LUNG CANCER

CANCER INITIATING CELLS (CICs)

EPITHELIAL TO MESENCHYMAL TRANSITION

AIM OF THE STUDY

MATERIAL AND METHODS

Pag.14

***IN VITRO* STUDIES**

CASE STUDY

CELL ISOLATION AND CULTURE

CELL ENRICHMENT

CALU-3 CELL CULTURE

IMMUNOPHENOTYPIC CHARACTERIZATION BY FACS ANALYSIS

IMMUNOCYTOCHEMICAL ANALYSIS

FLUORESCENCE IN SITU HYBRIDIZATION

ULTRASTRUCTURAL ANALYSIS

***IN VIVO* STUDIES**

**IMMUNOHISTOCHEMICAL ANALYSIS OF A HUMAN LUNG
ADENOCARCINOMA**

EXPERIMENTAL MODELS

MORPHOMETRICAL ANALYSIS OF TUMOUR XENOGRAPTS

IMMUNOHISTOCHEMICAL ANALYSIS OF TUMOUR XENOGRAPTS

FLUORESCENCE IN SITU HYBRIDIZATION

**ISOLATION AND *IN VITRO* EXPANSION OF NEOPLASTIC CELLS FROM
XENOGRAFT TUMOURS**

STATISTICAL ANALYSIS

RESULTS and DISCUSSION

Pag.26

STUDY POPULATION

***IN VITRO* STUDY**

CELL ISOLATION AND ENRICHMENT

FACS ANALYSIS

IMMUNOCYTOCHEMICAL ANALYSIS

FISH ANALYSIS ON ISOLATED TE_pCS

ULTRASTRUCTURAL ANALYSIS

EVALUATION OF EMT ACTIVATION

***IN VIVO* STUDIES**

**IMMUNOHISTOCHEMICAL ANALYSIS OF PRIMARY HUMAN LUNG
CANCERS**

EXPERIMENTAL MODELS

MORPHOMETRIC ANALYSIS OF TUMOUR XENOGRAFTS

CHARACTERIZATION OF TUMOUR XENOGRAFTS

RE-ISOLATION OF NEOPLASTIC CELLS FROM XENOGRAFT

TUMOURS

CONCLUSION

FIGURES

Pag.34

REFERENCES

Pag.50

Introduction

Lung Cancer

Epidemiology

Lung cancer is one of the most common cancers in the world, with the highest morbidity and mortality among malignancies disease.

A 2008 world cancer report issued by International agency for research on cancer (IARC) shows that lung cancer accounts for 16,5% of all new cancer cases, with a percentage of mortality of 22,5% respect to all cancer, confirming its as one of the leading causes of cancer-related mortality worldwide¹.

The population segment most likely to develop lung cancer is people aged over 50 who have a history of smoking. Although the relative incidence of lung cancer is decreasing, a recent study on cancer mortality in the countries of the European Union predicted in 2012 a decrease of mortality from lung cancer by 10% in males (while remaining the leading cause of death by cancer) but an increase by 7% in females (thus becoming the second leading cause of cancer mortality)².

This change is in part due to the different trend of smoking in both sexes of the last two decades, which shows a moderated increment of use of tobacco in females.

The prognosis for patients diagnosed with lung cancer is poor, with overall five year survival remaining below 15,7%. This is partly attributable to relatively ineffective methods for early detection and lack of curative treatment for advanced disease. The 5-year relative survival rate varies markedly depending on the stage at diagnosis, from 49% to 16% to 2% for patients with local, regional, and distant stage disease, respectively.

Etiology

Although the etiology of lung cancer is still partially unknown, inhaled carcinogens are known to be important predisposing causes. Particularly, about 83% of lung cancers are directly linked to smoking and inhaling the carcinogens in tobacco smoke³; the risk is higher with an increase of number of cigarettes smoked/day and earlier age of smoking.

However, numerous other substances, occupations, and environmental exposures have been linked to lung cancer, such as high levels of pollution, radiation, and asbestos.

Finally, individual differences in susceptibility to lung carcinogens may be the result of genetic predisposition to lung cancer⁴. Several evidences shows a correlation between a genetic predisposition, inherited or acquired during life, the exposure to certain environmental factors and the onset of lung malignancies.

Histology

Histologically, lung cancers are classified by the size and the appearance of the malignant cells in two main types: small cell lung cancer (SCLC) and non-small cell lung cancer (NSCLC)⁵. Mostly of lung cancers are carcinomas, malignancies that arise from bronchial epithelial cells.

SCLC represent about 15 percent of all lung cancers. This is an aggressive cancer made up by fast-growing small cells that can spread to other organs. Generally it starts in the bronchi, growing in the central part of the lungs. SCLC is more responsive to chemotherapy and radiation therapy than other cell types of lung cancer, but a definitive cure is difficult to achieve and the prognosis is closely linked to the extent of disease by time of diagnosis.

NSCLC represent the remaining 85 percent of lung cancer cases. NSCLC arises from the epithelial cells of the lung of the central bronchi to terminal alveoli. It generally grows and spread more slowly than SCLC. This class comprises three different histological subtypes which correlates both for the site of origin and the similar approaches to diagnosis, staging, prognosis, and treatment.

The three histological subtypes are:

- **Squamous cell carcinoma (SCC)** or epidermoid carcinoma represents 30 percent of lung cancers; this is a central tumor that usually starts near a central bronchus. Any of morphological features include intercellular bridges and individual cell keratinization. SCC is the most common type of lung tumor in men, smokers;
- **Adenocarcinoma (AC)** represents now the dominant histotype of all lung cancers (35%); it predominantly arises in peripheral lung tissue and is histologically characterised by the presence of glandular differentiation and/or mucin production, although often it shows a mixed histological pattern. AC is the most common type of lung cancer in women, nonsmokers;
- **Large-cell undifferentiated carcinoma (LCC)** represents approximately 10-15 percent of all lung cancers. LCC is a rapidly growing cancer arising near the outer edges or surface of the lungs. The LCC classification is seldom used today and has been replace by a more specific classification based on specific cancer cell type (such as *large cell neuroendocrine carcinoma*).

Clinical and therapeutical aspects

Therapeutical approaches for lung cancer are determined by histology, stage, and general health and comorbidities of the patient. The main lung cancer treatments are surgery, chemotherapy and radiation. Usually, this is no single treatment for lung cancer, but patients often receive a combination of therapies and palliative care.

Generally, surgery is performed for patients with resectable disease, classified on the size of the primary tumor, the potentially involvement of lymph node and metastases. The surgical resection of cancer can be followed by chemotherapeutic or radiation treatment.

For patients with unresectable disease the treatment with radiation and/or chemotherapy permits to treat localized lesions and may achieve long-term survival.

SCLC has the most aggressive clinical course of any type of pulmonary tumor; it responds well to chemotherapy and it is not generally treated with surgery. Today the standard of SCLC care is the combination of chemotherapy with thoracic radiation therapy (TRT): evidences show that TRT increases survival by approximately 5% over chemotherapy alone^{6,7}.

On the contrary, NSCLCs are relatively insensitive to chemotherapy and radiation therapy compared with SCLC. The elective treatment for early stage NSCLC is the complete excision of neoplastic mass that can be followed by chemotherapeutic or local radiation treatment.

A new era in the treatment of lung cancer started with the identification of genetic mutations in any subtypes of this cancer⁸. This discovery has led to the development of new molecular target therapy associated with specific cell types and subtypes. Targeted therapies are designed to only treat cancer cells. These include monoclonal antibodies, anti-angiogenesis agents and growth factor inhibitors that disallow the cancerous cells to grow.

In particular, genetic abnormalities of potential relevance to treatment choices are identified easily in NSCLC, in particular in a subset of adenocarcinoma. Among others, the most significant mutations found are:

- Specific mutations in genes encoding components of the epidermal growth factor receptor (EGFR)^{9,10};
- Translocations involving the anaplastic lymphoma kinase (ALK)-tyrosine kinase receptor, which are sensitive to ALK inhibitors¹¹;
- Amplification of MET (mesenchymal epithelial transition factor), which encodes the hepatocyte growth factor receptor.

These mutations may define mechanisms of drug sensitivity and primary or acquired resistance to kinase inhibitors: i.e MET amplification has been associated with secondary resistance to EGFR tyrosine kinase inhibitors¹².

The development of these new therapeutic strategies has improved the survival of lung cancer patient but prognosis is still poor. This is probably due to lack of knowledge of lung cancer biology and its carcinogenesis.

Human Stem Cells

It has been largely demonstrated the presence of a population of adult stem/progenitor cells (SC) in all human organs that is responsible for both maintenance of tissue homeostasis and repair tissue after injury.

SC population is capable of unlimited self-renewal and can develop into more differentiated cell types (pluripotential)¹³, but in normal condition its turnover is relatively slow. They are concentrated in protected areas of each tissue called niches. The stem cell niche comprises not only stem cells but also a number of other differentiated cell types, diverse extracellular matrix proteins (ECMs), and other growth factors; the adhesion between stem cells and more differentiated cells appears to be important for the self-renewal of stem cells, the maintenance of their pluripotential and their differentiation into mature cells¹⁴.

An alteration of niche micro-environment or a deregulation of intracellular pathway may compromise the physiological function of the organ. In particular, several studies have demonstrated that cancer stem cells exhibit many stem cell properties: this involves the possibility that carcinogenesis process may start from a stem/progenitor resident cell.

Human Lung Stem Cells

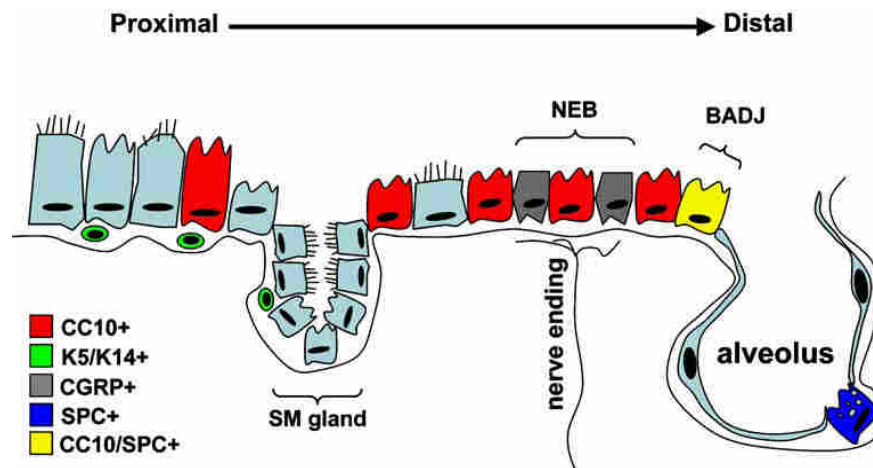
SC are found in a number of adult tissues, including the lungs¹⁵.

The lung is an organ anatomically complex, because is composed by multiple anatomic region, each characterized by a unique cellular organization and unique repair mechanism. So, also epithelial stem cell populations in the lung are classically subdivided by region¹⁶.

The most proximal conducting airways display a columnar epithelium constituted by ciliated cells, secretory Clara cells, basal cells, and submucosal glandular epithelium: the stem cell compartment in this area has been identified in the basal and parabasal cell.

In the distal bronchiolar airway there is an epithelial surface with no basal cells and an increasing ratio of secretory Clara cells, that are the stem compartment able to proliferate after injury.

At the broncho-alveolar duct junction the airway epithelium changes to organized into distal functional alveoli. These structures are formed by type I pneumocytes, that form the gas-exchange surface area of the lung, and cuboidal surfactant-expressing pneumocytes type II, which were identified as the stem compartment of this area of lung parenchyma.



Schematic representation of lung epithelial progenitor cells and their spatial location in the lung parenchyma.

Cancer stem cell and lung cancer

The classification of pulmonary SC above can reflect the specific parenchymal distribution of lung cancer and support the idea that oncogenesis process can be start from a normal resident stem cell.

Several studies suggest that pulmonary stem cell signaling and differentiation pathways are maintained within distinct cancer types, and that the destabilization of this signaling is related to the development of region-specific lung cancers.

In particular, in many experiment conducted with different murine models the lung cancer development seems to follow a proximal-to-distal distribution pattern: from the trachea to distal lung parenchyma, major tumor types include squamous cell carcinomas (SCCs), small cell lung carcinomas (SCLCs), and adenocarcinomas/bronchoalveolar carcinomas (AC). This regional segregation of lung cancer subtypes suggests that only specific cell populations and/or pulmonary environments are capable of supporting tumor growth¹⁷.

It was supposed that these different classes of cancer arise from specific resident stem cells located in restricted areas of lung parenchyma. For example, lung SCC, usually located on central part of the lung, is rich of basal elements recognized by CK5 expression and then it may derive from basal stem cell of trachea; also for AC, usually located in the distal bronco-alveolar district, there are evidences of its origin from the regional bronchioalveolar stem cells (BASCs)¹⁸.

From these literature data results necessary a better understanding of the relationship among stem cell regulation, cellular mutation, and lung cancer oncogenesis, especially to develop the next wave of lung cancer therapies.

Cancer initiating cell (CIC)

The first evidence of stem cells involvement in the genesis and progression of several cancer types have been observed in hematological, brain and breast malignancies^{19,20,21}.

In particular, recent studies^{22,23} have introduced the new concept of cancer initiating cells (CICs) referring to a subpopulation of cancer stem cell (CSC) pool that seems able to drive each step of tumor reprogramming, from the beginning of growth and metastasis, and showing radio- and chemotherapy resistance.

CICs were also identified for their capacity to generate *in vivo* a neoplasia with the same morphological features of the original tumor, proving their unique abilities to self-renewal and differentiate into all cell compartment necessary for tumor growth.

Despite of functional characterization of CICs, many other informations on their origin and molecular pattern are required to consider them as a target of cancer therapies. In particular, the identification of a reliable panel of markers for CSC and CIC populations, cancer and organ-specific, may lead to a better understanding of the pathogenesis of cancer and, considering the probable involvement of both population, CICs in particular, in cancer establishment to design a specific drug therapy against them.

Epithelial-To-Mesenchymal transition

The current knowledges on CICs and their dominant role in the cancer progression may explain the high aggressiveness and invasive potential of some cancer types.

In particular, in reference to lung cancer progression and metastasis, recent studies have related the invasive potential of cancer cells to activation of the Epithelial-to-

Mesenchymal Transition; on the other hand, the establishment of disseminated metastasis was associated to the inverse process of Mesenchymal-to-Epithelial Transition (MET)^{24,25}.

Assuming that mostly of lung cancers have an epithelial origin, the EMT/MET processes are thought to be an important mechanism for promoting cancer invasion and metastasis.

Epithelial cells are characterized by well-developed, intercellular contacts, whereas mesenchymal cells seldom form intercellular junctions.

For this reason, the EMT requires transcriptional reprogramming to downregulated expression of cell adhesion molecules and simultaneously to upregulated proteins involved in motile cell state characteristic of mesenchymal-like phenotype.

The EMT is a critical process activated during the embryonic development; if refers to adult differentiated epithelial cells and in particular to lung cancer progression, some differences have been reported.

For the lung cancer, two main hallmarks of EMT are loss of E-cadherin, a key mediator of cell–cell junctions and the increase of expression of the surface motile protein Vimentin. Numerous studies have related the inverse relation between these two markers and the gain of tumor invasiveness in cancer cells^{26,27,28}.

In particular, loss of E-cadherin appears to be a prerequisite for tumor progression and not just a consequence of tumor dedifferentiation. Some studies on experimental models show that during tumorigenesis, E-cadherin expression was shown to decrease with tumor progression, but it maintenance arrested tumor development²⁹.

Ectopic expression of E-cadherin results sufficient to suppress cancer cell invasion in vitro and in vivo, and the knock-down converts cell from non-invasive to invasive phenotype. However, the restoration of E-cadherin expression may be insufficient to reverse EMT and restore the epithelial phenotype. This imply that E-cadherin has a tumor suppressive function and is not simply a marker of tumor differentiation.

Furthermore, EMT activation was related to cell acquisition of stem properties³⁰ and also with a decrease of cell drug sensitivity^{31,32}; these two evidences confirm the hypothesis that a cancer cell undergo EMT process may become a metastatic drug-resistant cancer progenitor cell, or a metastatic CSC.

Aim of the study

Lung cancer remains the first cause of death among all human malignancies. Although the identification of several etiologic factors involved in this cancer development, the molecular and biologic mechanisms responsible of the beginning and the amplification of lung cancer cells are still partially unknown.

Recent studies have related the lung stem cell pool, physiologically responsible of maintenance of tissue homeostasis, to the cancer development, given that cancer stem cells present many features in common with the healthy stem compartment. In particular, a subpopulation of these cancer stem cell, called CICs, are responsible of cancer growth and metastasis; for these reasons, this population may be a new potential therapeutic target that may change the natural history of the lung tumor. Anyway, more investigation are necessary for a phenotypic characterization of CIC, related to cancer type.

A research project named “Lung Cancer-Initiating Cell” (LCIC) has made in our laboratory with the purpose of isolate and characterize a population of lung stem cells and lung cancer stem cells from human samples of subjects undergoing lobectomy for lung cancer. From cancer fragments, we have obtained several cell populations associated to stromal, endothelial and epithelial compartment of lung parenchyma.

In particular, this study was focused on the lung epithelial compartment: these cells cover the pulmonary surface of almost all districts of lung. For this reason, the lung stem cell niches comprise, among others, the epithelial stem cells, that are involved in the regeneration of epithelial compartment, but also in the cancer development. Indeed, almost all lung cancer have an epithelial origin.

On these evidences, this work shows the results relative to the isolation and characterization of an epithelial cell line isolate from a lung adenocarcinoma. The investigation of cell line properties was conduct in two steps: an *in vitro* characterization of cellular phenotype and growth characteristic, and an *in vivo* step to test the tumorigenic potential of this cell line through xenografts induction.

If the epithelial compartment is responsible of beginning and tumor progression, the possibility of isolate and characterize this cell compartment especially from more aggressive lung cancer may open new therapeutic options based on a personalized drug-therapy.

Material and Methods

The present investigation conforms with the National ethical guidelines (Italian Ministry of Health; D.L.vo 116, January 27, 1992) and the '*Guide for the Care and Use of Laboratory Animals*' published by the US National Institutes of Health (NIH publication no. 85-23, revised 1996). Specifically, informed consent was obtained from each patient to allow the collection of lung cancer samples.

In vitro studies

Case study

The study population consisted of 86 patients admitted to the Unit of Thoracic Surgery, University of Parma with lung cancer diagnosis and treated primarily with surgical resection of neoplastic area.

For the following analysis, lung tissue was collected and transported under sterile condition to the Department of Pathologic Anatomy, where it was sampled under hood at laminar flow by the medical staff. Particularly, from the resection were obtained portions of neoplastic and healthy tissue, that were put in sterile buffer in order to perform cell isolation.

Cell isolation and culture

Lung tissue fragments of 1-2 gr., obtained from lung cancer or distal parenchyma, were separately processed following the same protocol.

The tissue fragment was first minced using surgical scissors and after this first mechanical digestion the micro-fragments were digested in a solution of Accutase® (Sigma-Aldrich, Milan, Italy) for 75 minutes in a shaking bath at 37°C. At the end of enzymatic digestion, the tissue fragments were removed using a nylon filter with pores of 100 µm and the cell suspension was centrifuged at 240g for 5 minutes.

The pellet was then suspended in culture medium Dulbecco's modified Eagle's medium (DMEM) supplemented with 5% Fetal Bovine Serum (FBS, Sigma-Aldrich, Milan, Italy), 1% Penicillin-Streptomycin (P/S, Sigma-Aldrich, Milan, Italy), 1% Insulin-Transferrin-Sodium Selenite (I/T/S, Sigma-Aldrich, Milan, Italy), and specific growth factors as 10 ng/ml Basic-Fibroblast Growth Factor (b-FGF, Sigma-Aldrich, Milan, Italy), 10 ng/ml Epidermal Growth Factor (EGF, Sigma-Aldrich, Milan, Italy) and 1% Non Essential Amino Acids (NEAA) and seeded in 6 well plates at 37°C-5% CO₂.

Twenty-four hours after plating the debris and the non-adherent cells (erythrocytes, leucocytes, death cells) were removed by washing twice with PBS; fresh culture medium was then added to cell culture.

Cell monolayer was daily observed using an inverted microscope (Olympus CK40, Japan) and fresh culture medium was changed twice a week.

In the first week was observed an heterogeneous cell population mainly constituted of stromal and epithelial cells.

Cell enrichment

Tumor Epithelial Cells (TEpCs) were easily recognized by morphology and growth in colonies from the stromal adherent cells showing a fibroblast-like shape.

To obtain a pure population of both these cell lines we took advantage from their different resistance to Trypsin. The stromal population was more sensitive to trypsin activity and then was quickly and firstly removed by culture dishes. Then fresh enzyme was added to adherent TEpC to favour cells detachment from the dishes and their expansion.

The obtained suspensions of stromal cells and TEpCs were separately replaced in a new culture dish maintaining the growth condition previously described. The evaluation of cell growth was performed by daily observation and cell count.

Both these cell line were amplified for several passages and cryo-preserved in aliquots in a medium composed by FBS supplemented with 1% Dimethylsulphoxide (DMSO, Sigma-Aldrich, Milan, Italy).

Calu-3 cell culture

Calu-3 (ATCC[®] HTB-55[™]) is a bronchial epithelial cell line derived from a human lung adenocarcinoma of a 25 years-old caucasian male.

This cell line has been extensively researched and it was largely employed for in vitro and in vivo experimental model of respiratory system disease, including lung tumour.

Concerning this, the most important features of Calu-3 are the k-ras gene mutation, the amplification of the human epidermal growth factor receptor 2 (HER2/neu) while it was wild type for Epidermal Growth factor receptor (EGFR); also it was documented the absence of Y human chromosome in these cells.

Primary Calu-3 were purchased from American Type Culture Collection (ATCC[®] Milan, Italy) and cultured in tissue culture flasks with Dulbecco's modified Eagle's medium

(DMEM) supplemented with 10% Fetal Bovine Serum (FBS, Sigma, St. Louis, MO), 1% Penicillin-Streptomycin (P/S, Sigma, St. Louis, MO) and 1% Non Essential Amino Acids (NEAA) and placed at 37°C-5% CO₂.

The cell line was amplified and cryo-preserved at any passage in aliquots in a medium composed by FBS supplemented with 1% Dimethylsulphoxide (DMSO, Sigma, St. Louis, MO).

Immunophenotypic characterization by FACS Analysis

Fluorescence-Activated Cell Sorting (FACS) analysis is a fast and reliable method for characterizing and isolating specific cell subpopulations based on fluorescent labeling. One single analysis allows to collect several information on the entire population analyzed as cell number or mean dimension; it also permits the detection of specific biomarker and the sorting of a specific cell subpopulation from the initial pool.

For this study FACS analysis was performed on TEpC and stromal cell populations in order to evaluate the qualitative and quantitative expression of specific biomarker. Cells were harvested from culture flasks by trypsinization and suspended at density 1x10⁶ cells/ml in a simple sterile buffer.

At the cell suspension was added 1 µg/10⁶ cells of fluorochrome-conjugated (FITC or PE) monoclonal antibodies with determined specificity against stem cells antigens (CD117, CD133), mesenchymal (stromal) cell surface antigens (CD44, CD73, CD90, CD105), hematopoietic cell surface antigens (CD45), and the selective Epithelial-Cell Adhesion Molecule (EpCAM) a transmembrane glycoprotein expressed exclusively in epithelia and epithelial-derived neoplasms.

To test the cell vitality it was added to each cell suspension the DNA dyes 7-amino actinomycin D (7AAD), while for the negative controls was used a fluorochrome-conjugated antibody with irrelevant specificity.

The cell suspensions were incubated for twenty minutes at 4°C. Labelled cells were then washed with PBS to remove the exceed antibodies and centrifuged for six minutes at 240g at 4°C.

The pellet was analyzed by a FACS-Diva software. (FACSanto II) by acquiring at least 10,000 events.

The percentage of cells positive for each surface antigen (red line histograms) considered was obtained by subtracting the corresponding values of negative controls (green line histograms).

Immunocytochemical analysis

The immunocytochemical analysis on TEpC and Calu-3 cell lines was conducted on fluorescence and optical preparations. The two techniques diverge from each other for the revelation method.

For the fluorescence revelation is used a secondary antibody conjugated to a fluorochrome (Fluoresceine Isothiocyanate- FITC, Tetramethyl Rhodamine Isothiocyanate - TRITC or Cyanide 5 -CY5) and the nuclear counterstaining is performed with DAPI (4',6-diamidine-2-phenyndole, Sigma-Aldrich, Milan, Italy). Slides were mounted with fluorescence mounting medium Vectashield (Vector, USA).

For the optical preparation the secondary antibody is a peroxidase-conjugated streptavidin that catalyze the oxido-reduction reaction of the chromogenic substrate (DAB, 3-3' diaminobenzidin for 5 minutes). All sections were counterstained with Haematoxylin.

Immunofluorescence staining

In order to confirm the epithelial phenotype of the isolated TEpCs an immunocytochemical analysis was performed on this line and on Calu-3 as control line. The cells were cultured on 4-wells chamber slides and at 80% confluency slides were fixed with 4% paraformaldehyde, blocked, and permeabilized.

At first was performed an evaluation of specific epithelial antigens by staining for primary antibodies anti-E-cadherin (E-Cad, rabbit polyclonal, pre-diluted, Abcam, Cambridge, UK) and anti-panCytocheratin (panCK, mouse monoclonal, 1:20, 4°C o.n, DAKO).

It was also detected the expression of Mesenchymal/stromal surface antigens as Vimentin (Vim monoclonal mouse, 1:50, o.n. 4°, Millipore) and CD44 (rat monoclonal, 1:50, 4°C o.n, SantaCruz Laboratories)

The presence of the surface antigens was revealed through the conjugation with anti-mouse and anti-rabbit FITC-conjugated secondary antibodies (1:70 60' 37°C, Sigma-Aldrich).

TRITC-conjugated secondary antibody was employed to detect the CD44 expression (anti rat, 1:70 60' 37°C, Sigma-Aldrich).

Nuclei were counterstained by DAPI and cover slips mounted with Vectashield.

Immunoperoxidase staining

In order to confirm the pulmonary origin of these lines, the expression of the nuclear transcription factor Thyroid Transcription Factor 1 (TTF-1, rabbit monoclonal, 1:20 4°C o.n., Abcam) was also detected by immunoperoxidase staining.

After trypsinization, cell suspension was fixed with 4% paraformaldehyde for 40 minutes, then the cells were suspended in a volume of buffer solution to obtain a density of 10^5 cells per spot. A cytofunnel was attached to a glass slide and slide carrier. The entire apparatus was inserted into a cytocentrifuge and the cell suspension was added and centrifuged at 240g for 5 minutes.

The cell spot was then stained for anti-TTF1 antibody and then revealed by DAB reaction.

Fluorescence In Situ Hybridization

Fluorescence In Situ Hybridization (FISH) is a cytogenetic technique that combine fluorescence microscopy to molecular methods of in situ hybridization. FISH is used to detect and localize specific DNA sequence or chromosome, included sexual X and Y chromosome; for this purpose a fluorescent probe complementary to DNA researched sequence is used.

For cytological staining, the cell population was cultured in a 4-well chamber slide until 80% confluency; then it was first fixed with 4% paraformaldehyde and pre-treated with saline solution of Saline Sodium Citrate buffer (SSC) 2x at double boiler for 30 minutes at 80°C. After the preparations were wash-out twice with SSC 2x buffer and finally a dehydration with alcohol- increasing concentration of section was conduct before the addition of molecular probe.

Specifically, for research of human sexual chromosomes was used a mix of two human specific Chromosome Enumeration Probe (CEP), complementary to centromeric region of X chromosome (Alpha-Satellite DNA, locus X p11.1-q11.1, Vysis, USA) and Y chromosome (Satellite III DNA, locus Yq12, Vysis, USA).

The specific hybridization protocol for these probes was performed with a HYBrite instrument and imply a first denaturation step of 10 minutes at 90°C and an overnight hybridization step at 42°C. After hybridization, samples were washed-out in SSC 2x buffer solution and a formamide solution at 42°C. The nuclei were counterstained with DAPI.

The analysis was performed with a fluorescence microscope Olympus BX60.

Ultrastructural Analysis

Cell lines of TEpC and Calu3 were also analyzed by Transmission Electron Microscopy (TEM) to detect structural and subcellular features.

After trypsinization, both cell populations were fixed in Karnovsky solution (4% formaldehyde, 5% glutaraldehyde) for 90 minutes at room temperature. After washing with several changes of 0.1M phosphate buffer, PH 7.2, the pellets were embedded in agar to maintain themselves cohesive for the successive passages.

The samples were postfixed in 1% osmium tetroxide (OsO₄) for 90 minutes at room temperature and dehydrated by increasing concentration of alcohol. Following this procedure, samples were washed with propylene oxide and embedded in epoxy resin. Sections of 0.5 µm thickness were stained with methylene blue and safranin to select morphologically the field of interest. Subsequently, ultrathin sections were collected on a 300-mesh copper grid and, after staining with uranyl acetate and lead citrate, were qualitatively examined under a transmission electron microscope (Philips EM 208S).

In vivo studies

Immunohistochemical analysis of a human lung adenocarcinoma

In order to evaluate the effective epithelial origin of the TEpCs population obtained from lung adenocarcinoma, the histological case of interest was analyzed by immunohistochemical staining.

Five-micrometer-thick sections obtained from formalin-fixed paraffine-embedded lung fragments were analyzed under fluorescence microscopy to determine the qualitative expression of specific surface and nuclear antigens already detected on isolated TEpCs.

After sections deparaffination in Xylene and in a decreasing concentration of ethanol, rehydration and antigenic unmasking through a pre-treatment in citrate buffer (pH=6) by microwave, the samples were stained with several primary antibodies such as anti-E-Cad (rabbit polyclonal, prediluted, 4°C o.n., Abcam), anti-CD44 (rat monoclonal, 1:100, 37°C 90 minutes, SantaCruz Laboratories), anti-panCK (mouse monoclonal, 1:50, 37°C 90 minutes, DAKO) and anti-Vim (monoclonal mouse, 1:50, o.n. 4°C DAKO).

Also the research of the mitosis marker Phosphohistone-H3 (pH3, rabbit polyclonal, 1:100 o.n. 4°C, Upstate, Lake Placid, NY, USA) was performed to evaluate the ratio of proliferating tumoral pan-CK^{POS} population.

The presence of the surface antigens was revealed through the conjugation with anti-mouse and anti-rabbit FITC-conjugated secondary antibodies (1:70 60' 37°C, Sigma-Aldrich). TRITC-conjugated secondary antibody was employed to detect the CD44 expression (anti rat, 1:70 60' 37°C, Sigma-Aldrich) and also panCK (anti mouse, 1:70 60' 37°C, Sigma-Aldrich). Nuclei were counterstained by DAPI and cover slips mounted with Vectashield (Vector, USA)

Experimental models

In order to test the tumorigenic potential of isolated TEpCs and Calu3, a subcutaneous injection of these cell populations was administered in Balb-c NUDE female mice (CAnN.CG-Foxn1^{nu}/CrI, Strain Code 194 Homozygous, Charles River Laboratory, Calco, Italy).

Each animal was anaesthetized with a inhalation of vapour of ether; the cell pools were suspended in a saline buffer at the final density of 10⁶ cells/each animal; this solution was added to an equal quantity of Matrigel[®] (BD Bioscience, Franklin Lakes, NJ) and subcutaneously injected on the right flank of each mouse using a 1ml-syringe.

A solid tumor was generated only in correspondence of the injection site. The growth of each tumor was evaluated by measuring tumor volume twice a week until animals sacrifice. The tumour volume was determined by the equation $(\text{lenght} \times \text{Widht}^2) \times 0,5$.

The animals were sacrificed approximately five weeks after tumor induction by cervical dislocation; the tumors were collected for both cell isolation and histological assessment.

Morphometrical analysis of tumour xenografts.

After paraffin inclusion, from the tumoral nodules were obtained five-micrometer-thick sections stained with Haematoxylin and Eosin (H&E), Masson's Trichrome or used for immunohistochemistry.

In order to compare the histological features of xenograft tumors with the primary human cancer an histological evaluation with H&E stained was performed.

On the sections stained by Masson's Trichrome was also made the morphometric evaluation of nodules composition in terms of area occupied by collagen or neoplastic formation. Microphotograph of total nodule were captured by an optical microscope connected to a digital camera with final magnification of 40X. Subsequently, the area occupied by collagen deposition or neoplastic tissue was evaluate by image analysis software (Image pro-plus 4.0, Media Cybernetics, USA). A macroscopic image of the whole nodule was captured to determine the total area.

Moreover, for the neoplastic tissue was also obtain the percentage of glandular and luminal area respect to the total neoplastic area

Immunohistochemical analysis of tumour xenografts.

Additional data about the morphological features of both induced- and human cancers were also produced by immunohistochemical detection of surface and nuclear antigens described above in order to compare the tumoral and stromal organization of tumor xenografts with the primary human cancer.

Five-micrometer-thick sections obtained from formalin-fixed paraffine-embedded samples were analyzed under fluorescence microscopy to determine the qualitative expression of specific surface and nuclear antigens already investigated on isolated TEPs.

After sections deparaffination in Xylene and in a decreasing concentration of ethanol, rehydration and antigenic unmasking through a pre-treatment in citrate buffer (pH=6) by

microwave, the samples were stained with several primary antibodies such as anti-E-Cad (rabbit polyclonal, pre-diluted, 4°C o.n., Abcam), anti-panCK (mouse monoclonal, 1:50, 37°C 90 minutes, DAKO), anti-CD44 (rat monoclonal, 1:100, 37°C 90 minutes, SantaCruz Laboratories) and anti-Vim (monoclonal mouse, 1:50, o.n. 4°C DAKO).

Also for the xenografts the detection of the mitosis marker Phosphohistone-H3 (phH3, rabbit polyclonal, 1:100 o.n 4°C, Upstate, Lake Placid, NY, USA) was performed to evaluate the ratio of proliferating tumoral pan-CK^{pos} population.

The presence of the surface antigens was revealed through the conjugation with anti-mouse and anti-rabbit FITC-conjugated secondary antibodies (1:70 60' 37°C, Sigma-Aldrich). TRITC-conjugated secondary antibody was employed to detect the CD44 (anti rat, 1:70 60' 37°C, Sigma-Aldrich) and panCK (anti mouse, 1:70 60' 37°C, Sigma-Aldrich) expressions.

Nuclei were counterstained by DAPI and cover slips mounted with Vectashield (Vector, USA)

Fluorescence In Situ Hybridization

FISH analysis for the detection of human sexual chromosomes was used to tracking the injected human cells in the tumour xenograft samples.

Respect to the FISH protocol described above for the cell samples, the use of this technique on paraffin-embedded sections requires appropriate protocol devices.

The first step for these samples is the deparaffination in Xylene and in a decreasing concentration of ethanol with subsequent rehydration. The sections were then process by acid hydrolysis with HCl 0,2N for 20 minutes at room temperature and pre-treated with a saline solution of Saline Sodium Citrate buffer (SSC) 2x at double boiler for 30 minutes at 80°C. Subsequently, in order to denature cellular proteins and promote the binding of nucleic acid to hybridization probe, an enzymatic digestion with Proteinase K was performed at 37°C. Finally, a post fixation with 4% formaldehyde and alcohol dehydration of section was conduct before the addition of molecular probe.

For research of human sexual chromosomes was used a mix of two human specific Chromosome Enumeration Probe (CEP), complementary to centromeric region of X chromosome (Alpha-Satellite DNA, locus X p11.1-q11.1, Vysis, USA) and Y chromosome (Satellite III DNA, locus Yq12, Vysis, USA).

The specific hybridization protocol for these probes was performed with a HYBrite instrument and imply a first denaturation step of 10 minutes at 90°C and an overnight

hybridization step at 42°C. After hybridization, samples were washed-out in SSC 2x buffer solution and a formamide solution at 42°C. The nuclei were counterstained with DAPI.

The analysis was performed with a fluorescence microscope Olympus BX60 at 100x magnification with oil immersion objective.

Isolation and *in vitro* expansion of neoplastic cells from xenograft tumours.

After tumor excision, part of each nodule was utilized for the re-isolation of tumor injected cells. The tumoral nodules were excised in sterile condition and processed separately for each group (Calu-3 or TEpC cell injection) under hood at laminar flow.

After removal of surrounding epidermal and connective tissue, one-half of each nodule was fixed in 4% formaldehyde, while the remain part was washed-out with a saline buffer and then processed for the cell isolation.

As for the human lung fragments, nodules were firstly minced with scissors and then put into a collagenase/dispase solution (C/D, 1mg/ml, ROCHE) for 40 minutes in a shaking bath at 37°C. At the end of enzymatic digestion, the tissue fragments were removed using a nylon filter with pores of 100 µm and the cell suspension was centrifuged at 240g for 5 minutes.

For the cells rescued from the nodules formed by Calu-3, the medium culture was Dulbecco's modified Eagle's medium (DMEM) supplemented with 10% FBS, 1%, P/S, 1% I/T/S and 1% NEAA. On the other hand the pellet obtained from TEpC nodules digestion was suspended in complete DMEM medium supplemented with specific growth factors as 10 ng/ml of b-FGF and 10 ng/ml of EGF. Both cell suspension were seeded in 6 well plates at 37°C-5% CO₂.

Twenty-four hours after plating the debris and the non-adherent cells were removed by washing twice with PBS; fresh culture medium was then added to cell culture and then changed twice a week.

Daily observation of cellular monolayers using an inverted microscope (Olympus CK40, Japan) pointed out the growth of two different adherent cell populations, one with fibroblast-like shape and one with epithelial characteristics.

Statistical analysis

The SPSS statistical package was used (SPSS, Chicago, IL, USA). Normal distribution of variables was checked by means of the Kolmogorov-Smirnov test. Statistics of variables included mean \pm standard error (S.E.M.), paired Student t-test, one-way analysis of variance (post-hoc analyses: Bonferroni test or Games-Howell test, when appropriate). Statistical significance was set at $p < 0.05$.

Results and Discussion

Study Population

The patient population consisted of 86 subjects undergoing lobectomy for lung cancer.

All samples recruited for the study were classified by diagnosis and histopathology of the disease, sex, age and smoking status (*Table 1*). The diagnosis performed by pathologists documented 52 Adenocarcinoma, 22 Squamous cell carcinoma (SCC) and 12 Neuroendocrine tumor samples.

Related to sex incidence, our data show an equal incidence of neuroendocrine carcinoma for both male and female whereas the other two histological subtypes show dominant incidence in male sex, especially SCC, that seems strictly related to smokers status more than adenocarcinoma.

Histology	Nr Tot	Male	Female	Age, years	Smoker
Adenocarcinoma	52	34	18	68	18, 28 ex
Squamous Cell Carcinoma	22	21	1	67	9, 13 ex
Neuroendocrine Carcinoma	12	6	6	62	4, 5 ex

Table 1 Case Study Classification

In vitro study

Cell isolation and enrichment

After the mechanical and enzymatic digestion of healthy and neoplastic tissue we have obtained an heterogeneous population of adherent cells that we could expand *in vitro* for several passages. In particular basing on their morphologies we have identified two main populations: a stromal pool with a fibroblast-like morphology, and one with the classical epithelial morphology (Figure 1A).

The stromal population was easily maintained and expanded *in vitro*: these cells grow quickly and reach confluence approximately five days after plating. Both healthy and tumor stromal cells were phenotypically characterized by FACS and immunocytochemical analysis (data not shown).

The epithelial population was obtained from cancer nodule. In relation to lung cancer type, the isolated morphologies were different for shape and growth characteristic (Figure

1B,C). Generally, all these epithelial populations grow in colonies and slowly when compared to stromal lines.

Although the isolation protocol seems to be appropriate for the cell isolation from several lung cell compartments, the expansion and maintenance of epithelial cells in culture require some adjustments.

Anyway we were able to expand and characterized one of these epithelial cell lines, derived from a lung adenocarcinoma of a 58-years old male (Figure 2A).

In particular, the patient is an 12-years ex-smoker (90 pack/year); he was submit to right inferior lobectomy with a diagnosis of lung mucinous-type adenocarcinoma, classified after histological analysis at pT1aN2 pathological status, staging IIIa. The patient was no affected by previous malignancies and no treated with neoadjuvant chemotherapy.

The isolated cells were compared to Calu-3 population for their similar epithelial and cancer origin (Figure 2B). A preliminary evaluation of cell growth show an equal exponential trend, even if TEpCs are fewer than Calu-3, probably due to different cell doubling time (Figure 2C, D).

FACS analysis

The epithelial nature of isolated TEpCs was first evaluated by FACS analysis at fourth passage of expansion (p4): the expression of EpCAM was detected in 95% of analyzed cells. Moreover, TEpC expressed the stem cell marker CD133 (35%) and the mesenchymal adhesion molecule CD44 (88%). Low or none positive cell for CD117 and mesenchymal markers were detected, except for CD73 (85%) (Figure 3).

Immunocytochemical analysis

More evidences of epithelial nature of TEpCs were obtained by immunocytochemical staining for specific epithelial markers such as panCK and E-Cad. Their expression was detected on the surface of almost all cells, especially in growing colonies (Figure 4A, B).

The mesenchymal markers Vimentin and CD44 were evaluated to assess if the *in vitro* culture conditions could influence the EMT process. Vimentin expression in TEpCs at p4 was detected only in few cells grown isolated from colonies whereas the adhesion molecule CD44 was localized on a high fraction of adherent cells, according to FACS analysis (Figure 4C, D).

The lung epithelial origin was confirmed by TTF-1 nuclear expression revealed by immunoperoxidase staining (Figure 4E).

These qualitative analysis were performed simultaneously in Calu-3: this cell line has the same source of isolated TEpC and then was used as positive control. The epithelial and mesenchymal markers show a similar quantitative and qualitative pattern distribution in both cell lines. Only the CD44 staining show a preferential expression surrounding the cell colonies. (Figure 5 A-E)

FISH analysis on isolated TEpCs

One of the characteristic of aggressive neoplastic cells is the presence of genetic anomalies; in particular, for the cell lines deriving from male patient, an extended proliferation causes the loss of Y sex chromosome and subsequent X-polysomy. The Calu-3 cell line of NSCLC characteristically displays this genetic tract (Figure 6B).

FISH analysis on our primary culture of TEpC at p4 passage was performed to evaluate potential sex chromosomes abnormality (Figure 6A). Our results shows that 90 % of TEpC carry X and Y chromosomes and only 10% of cells Y chromosome was undetectable.

Ultrastructural analysis

TEM analysis of cultured cells allowed us to evaluate their specific ultrastructural features.

TEpC and Calu3 appear similar in terms of shape and subcellular characteristic such as nuclear chromatin condensation and the presence of numerous intracytoplasmic vesicles; cell dimensions were slightly increased in Calu-3 compared to TEpC (Figure 7A-D)

In both cell preparations we were able to document one of the ultrastructural features of adenocarcinoma “signet ring” consisting of a large intracytoplasmic empty vesicle (Figure 7E, F).

Moreover, mitotic figures were found in TEM samples, as an additional feature of the high replicative capacity of neoplastic cells (Figure 7G,H).

Although cells have been treated with trypsin to obtain TEM samples, some adherent intercellular junctions were still present and well observable at higher magnification (Figure 8).

Evaluation of EMT activation

In order to evaluate if the *in vitro* amplification and expansion induced phenotypic changes in isolated TEpC, the cytofluorimetric and immunocytochemical analysis were performed on cultured cells at higher passages (p14). Data were compared to that obtained at p4.

The quantitative FACS analysis shows a slight reduction on the expression of the epithelial marker EpCam (90% versus 95% of p4) and of the mesenchymal-like marker CD44 (75% vs 88% p4). A significant increase from 35% at p4 to 73% at p14 was measured in the stem/progenitor marker CD133, and in the mesenchymal marker CD105 that was expressed by almost half of analyzed population at p14 (Figure 9).

The ICC staining for all markers described above shows similar results to those previously described, except for the increasing expression of fibroblast surface antigen Vimentin and the simultaneous decrease of epithelial marker EpCam expression. These observation taken together may be explained by *in vitro* activation of EMT process (Figure 10 A-E).

***In vivo* studies**

Immunohistochemical analysis of primary human lung cancers

In order to confirm that the TEpCs isolated from fresh lung cancer derive from epithelial cancer cell we have analyzed the histological samples of the specific clinical case (Figure 11A,B)

The specific epithelial markers E-Cad and panCK, highly expressed in the cytologic samples, have been largely detected also in histological preparations specifically in the epithelial cells that form the neoplastic glands (Figure 11C, D). The stromal markers CD44 is clearly expressed by neoplastic glands, while Vimentin was predominantly present in the peritumoral stroma (Figure 11E).

Several mitotic figures of epithelial cells were documented by double staining for pH3 and panCK (Figure 11F).

Experimental models

One of the principal features of a defined Cancer Initiating Cell (CIC) population is the tumorigenic potential, in other word their capacity to regenerate a neoplastic mass histologically equal to the original ones in several serial xenografts.

Experimental models of xenografts allowed us to test this property for isolated TEpCs, whereas for Calu-3 population it was largely documented^{33,34}.

After the injection of the same number of TEpCs and Calu-3 cells, the tumor growth was evaluated twice a week from the injection to animal sacrifice. The tumor volume initially decreased due to Matrigel[®] reabsorption. Then, both types of neoplastic cells gave rise to a solid mass with a similar size (Figure 12A-E).

Morphometric analysis of tumour xenografts.

A morphometric evaluation of tumour mass was assessed by H&E and Masson's trichrome staining. The nodules generated by Calu-3 and TEpC cells showed the typical glandular feature of adenocarcinoma clearly seen in histologic samples (Figure 13A-D).

The evaluation of tumour composition on sections stained with Masson's trichrome revealed that TEpC nodules were composed of 31% by connective tissue and 68% by neoplastic structures; the latter was further subdivided in glandular and luminal area, that occupy 92% and 4% of tumor area, respectively. When compared to TEpC xenografts, the

morphometric analysis of Calu-3 nodules showed an increased collagen deposition (56%) and a subsequent reduction of tumor area (43%), which was composed of epithelial cells (83%) and luminal area (16%) (Figure 13E,F).

Characterization of tumour xenografts.

On sections from nodules excised from both experimental groups, immunohistochemical and FISH analysis were performed in order to compare tumour xenografts with the primary lung cancer.

In particular, the IHC analysis of xenograft sections was performed to confirm that the solid mass excised from nude mice was a tumor generated from injected human cells with an adenocarcinoma provenance.

Compared with the clinical case, an equal distribution pattern of both epithelial and stromal markers was observed in the TEpC nodules (Figure 14A-D).

An additional evidence of human origin of induced tumor was obtained from the FISH analysis for human sex chromosomes. The typical X polysomy associated to Calu-3 and the presence of XY chromosomes in TEpC generated xenografts were detected in cells constituting the glands of adenocarcinoma. The double staining of sex chromosomes and panCK confirmed the original phenotype of the injected populations (Figure 14E).

The analysis performed in parallel with Calu-3 xenografts, documented a similar morphologic features of two induced tumours (Figure 15A-C).

Re-isolation of neoplastic cells from xenograft tumours.

Another step to prove the tumorigenic potential of TEpCs is the serial re-isolation and re-injection of cells from xenografts. For this purpose, a small fragment from each nodule of both experimental groups was processed for cell isolation.

The enzymatic digestion allowed us to obtain two main populations, one fibroblast-like of murine origin and one with epithelial morphology similar to injected cells (Figure 17A, B).

The expansion of these two populations is ongoing; obviously, both epithelial populations must be tested for their immunophenotypic properties and ability to generate tumours in secondary transplants.

Conclusion

The aim of our study was to identify and isolate a subpopulation of cancer initiating stem cells that is responsible of the maintenance and growth of the tumour. CICs can be recognized principally for their functional properties of self-renewal, aggressiveness and ability to sustain the cancer growth and metastasis. Furthermore, they are able to regenerate *in vivo* a neoplasia with the same phenotypic characteristics of the primitive cancer. This capacity implies the activation of molecular and genetic tissue-specific mechanisms which are responsible for the onset and progression of tumours.

Our attention was focused on one of the most aggressive human malignancies, the lung cancer.

The poor prognosis usually related to this cancer is likely due to the lack of knowledge of its pathogenetic bases and therefore the therapeutic approach is quite frustrating.

Preliminary data obtained from our study seem promising. Compared with a control cancer line Calu-3, the cancer epithelial cells isolated from a human primary adenocarcinoma showed an high grade of similarity, both phenotypic and functional.

In particular, the *in vitro* phenotypic changes in relation to epithelial and mesenchymal markers expression may be investigated in order to understand the signaling pathways and the micro-environmental factors implicated in epithelial-to-mesenchymal transition.

In regard of the functional properties, the experimental model of xenografts have confirmed that the isolated cancer pool possess a tumorigenic potential. The strong histotypic similarities of xenografts with the primary lung cancer reinforce our initial hypothesis of the stem epithelial nature of the isolated population. Moreover, the TEpC-induced xenografts were integrated with the stromal murine compartment.

In conclusion, the isolation and *in vitro* expansion of a primary lung cancer cell lines may be the first step for the characterization of a CICs subpopulation responsible of cancer progression. Its identification in lung cancer may have two potential implications: on one hand the possibility to develop a personalized therapy with new drugs highly specific for this subpopulation; on the other hand the phenotypic characterization of these cells could be the first step for their selective isolation followed by *in vivo* tumorigenic properties and studies on their molecular and genetic profile.

Figures

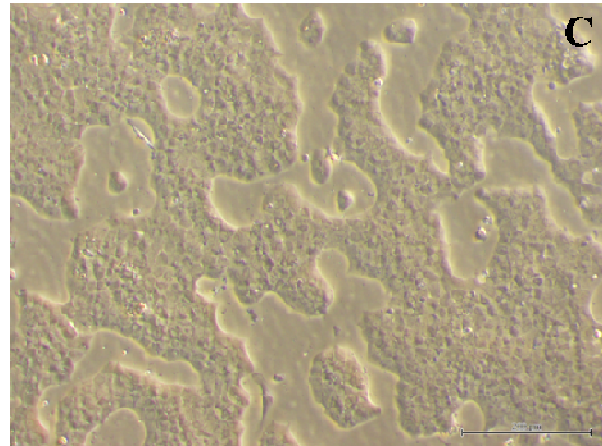
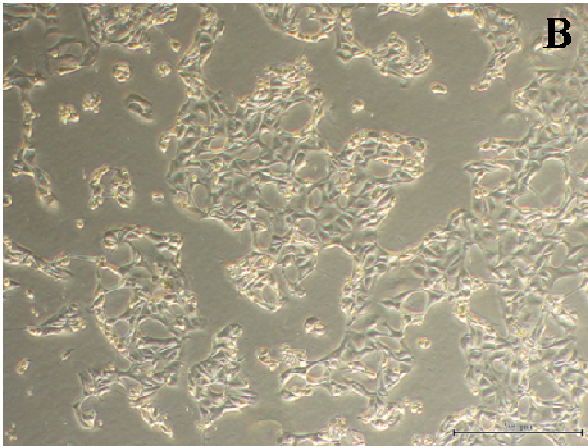
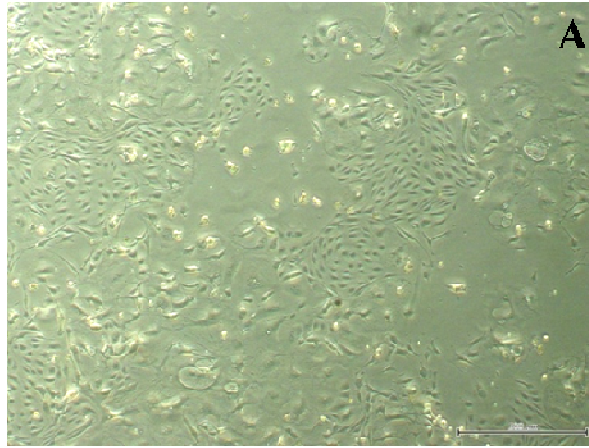


Figure 1: Phase contrast images showing the heterogeneous population (A) of adherent cells obtained from lung cancer fragments. Different morphologies of epithelial cells isolated from neoplastic lung fragments are shown in panel B and C. Scale bars A and B :500 μm ; C: 200 μm

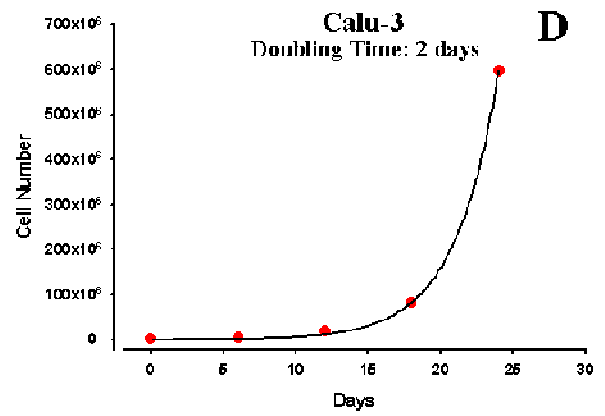
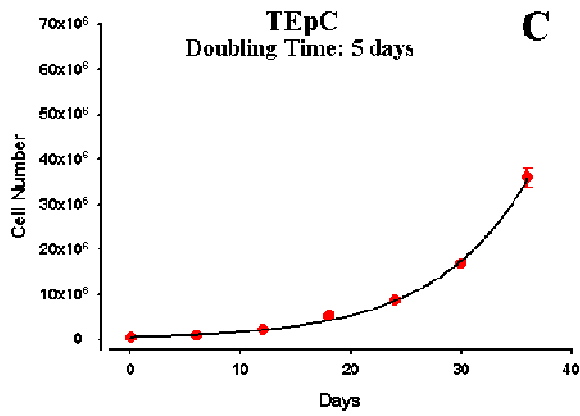
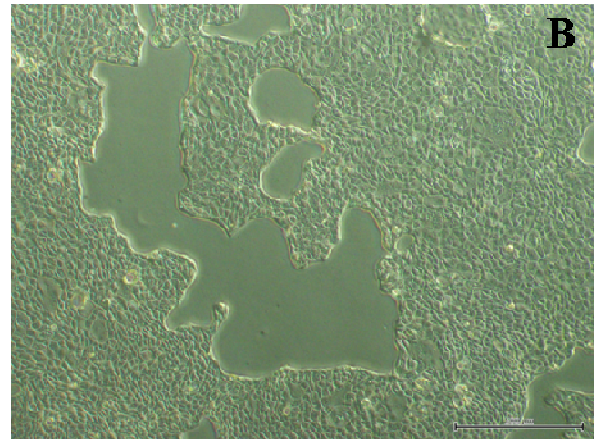
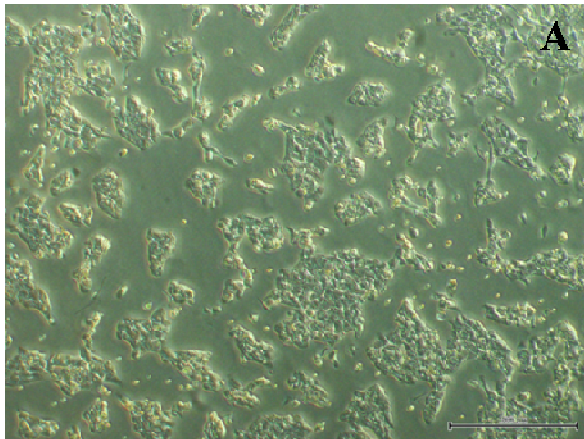


Figure 2: Tumour Epithelial Cell (TEpC) population isolated from a human lung adenocarcinoma (A). Calu-3 cell line is shown in B as control. Graphs show *in vitro* evaluation of cell growth of TEpC (C) and Calu-3 (D). Scale bars 500 μ m

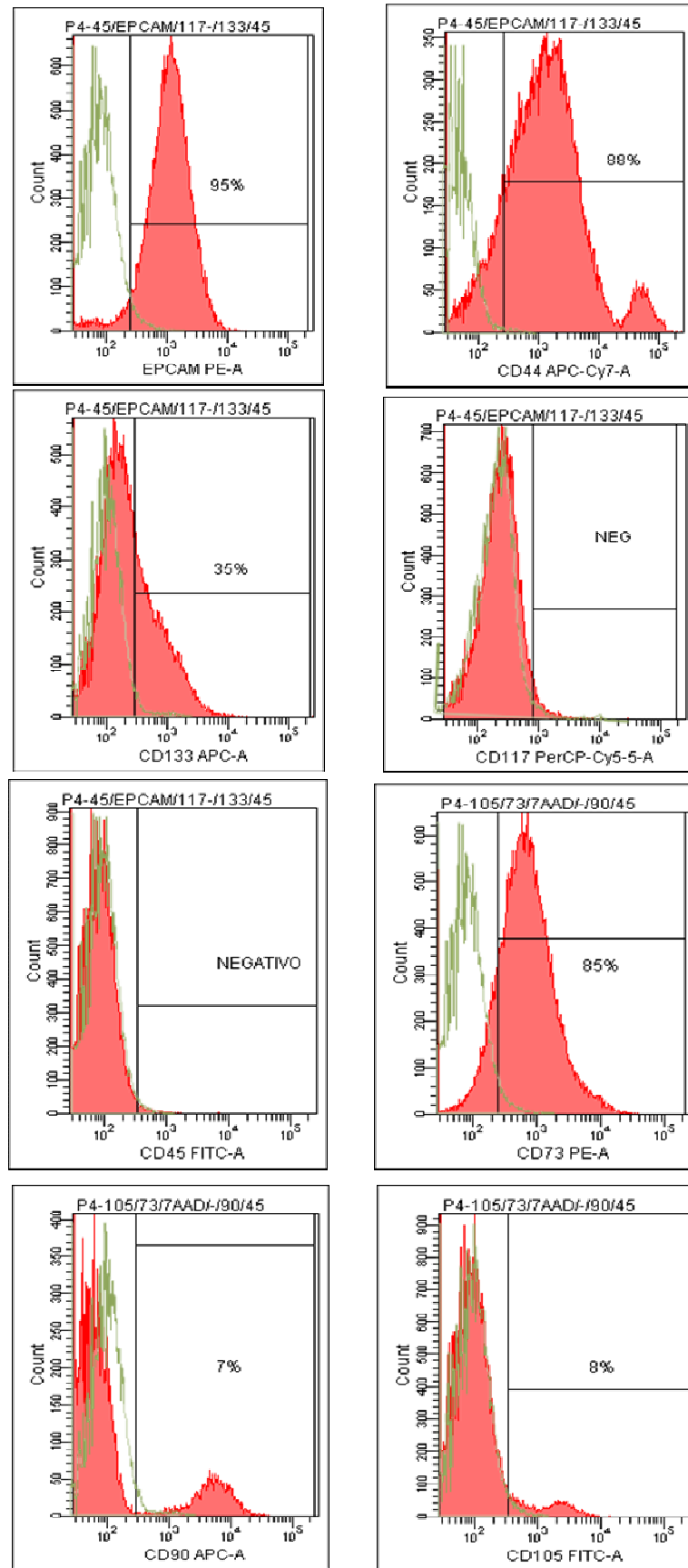


Figure 3: FACS analysis on TEpC at passage 4 of *in vitro* amplification

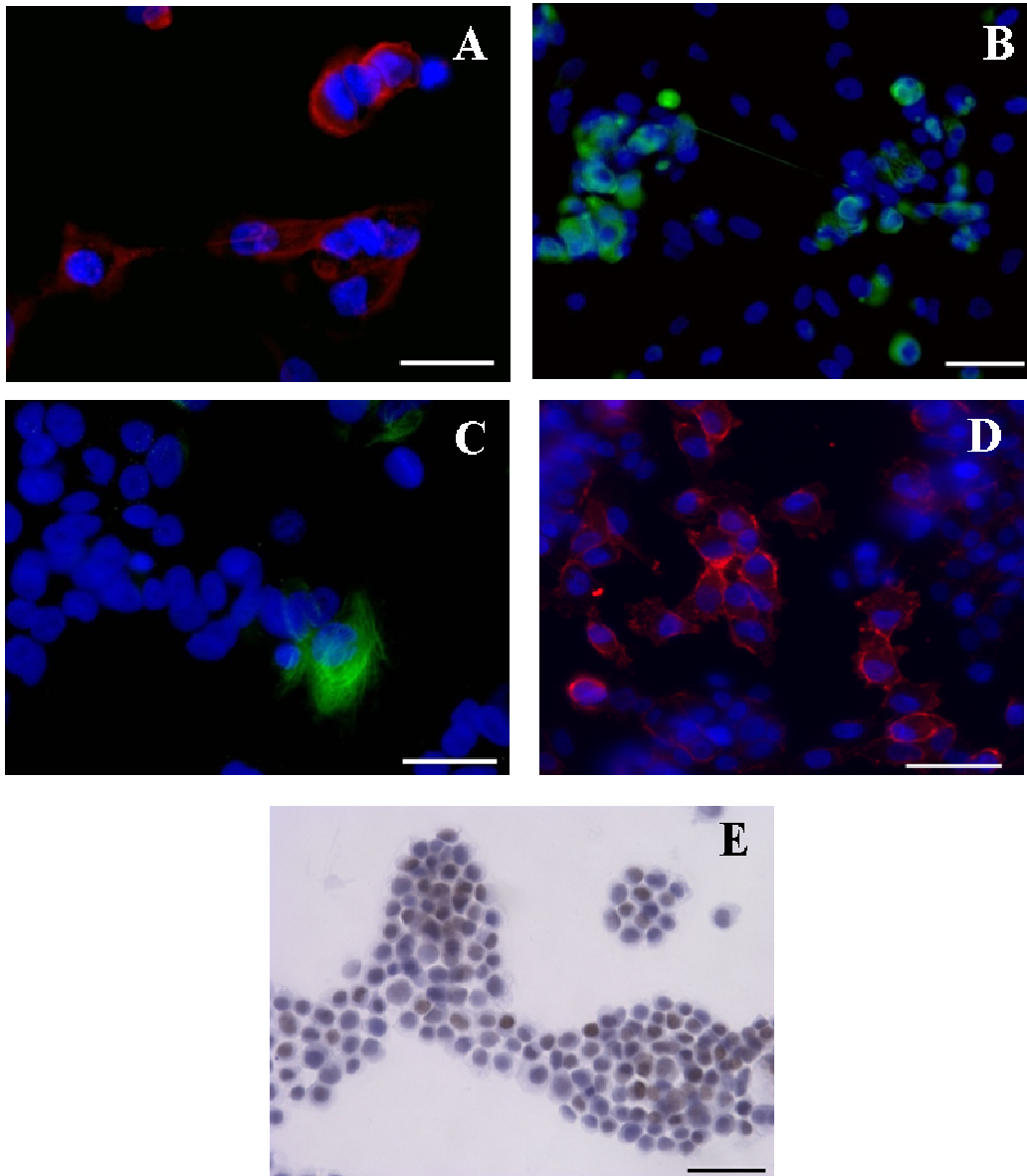


Figure 4: Immunocytochemical analysis of isolated TEPCs. The expression of epithelial markers E-Cad shown in red fluorescence (A) and panCK (green fluorescence, B) was present in almost all cells. The mesenchymal markers Vimentin (C) and CD44 (D) are also shown by green and red fluorescence, respectively. Nuclei are recognized by the blue fluorescence of DAPI.

The lung transcription factor TTF-1 is documented by immunoperoxidase staining (E).
 Scale bars A and C 30 μ m; B, D and E: 50 μ m

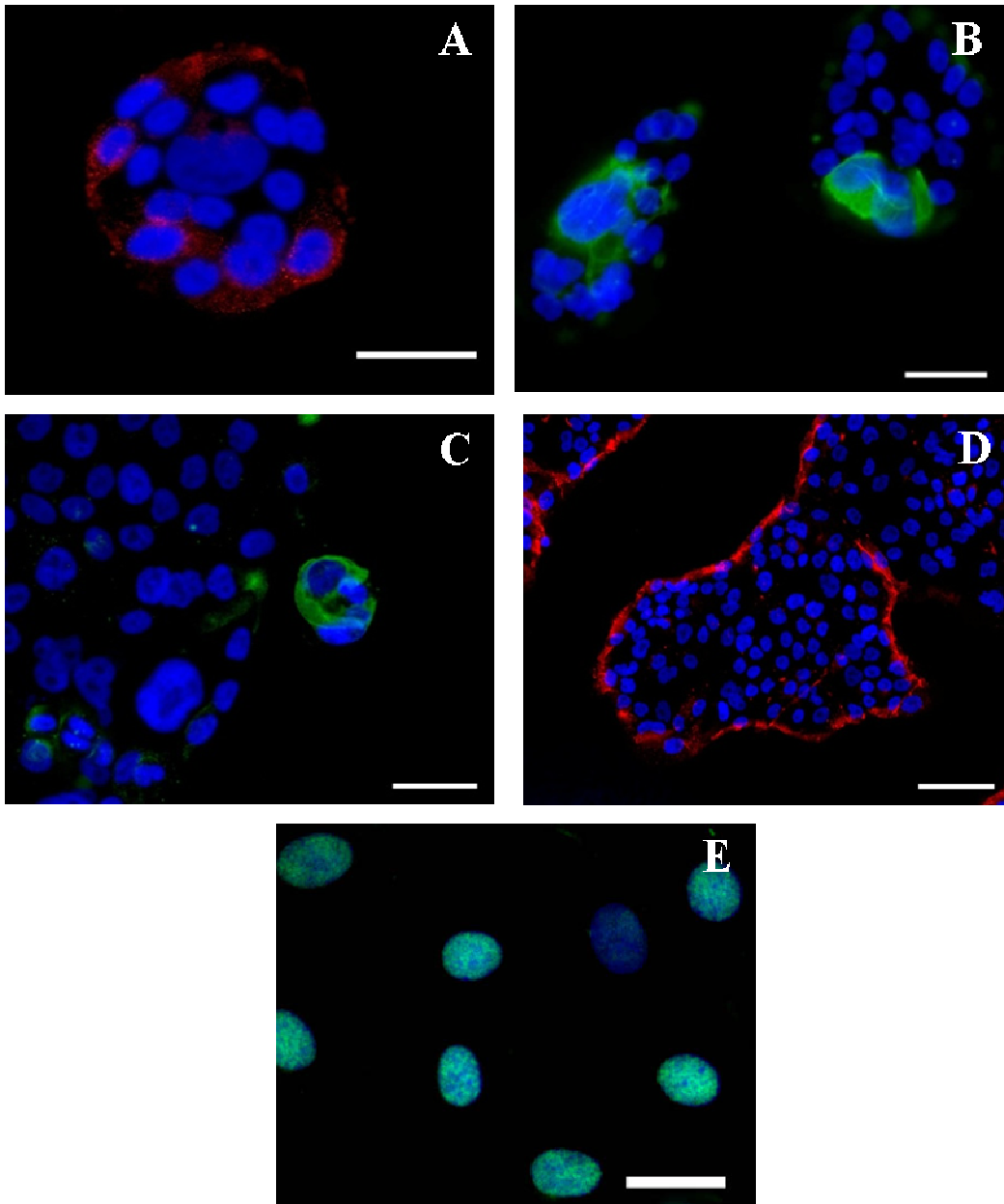


Figure 5: Immunocytochemical analysis of Calu-3. The expression of epithelial markers E-Cad shown in red fluorescence (A) and panCK in green fluorescence (B) was detected on almost all cells. The mesenchymal markers Vimentin (C) and CD44 (D) are also shown by green and red fluorescence, respectively. The lung transcription factor TTF-1 is shown by green fluorescence (E). Nuclei are recognized by the blue fluorescence of DAPI. Scale bars A, B, C and D :50 μm ; E :30 μm

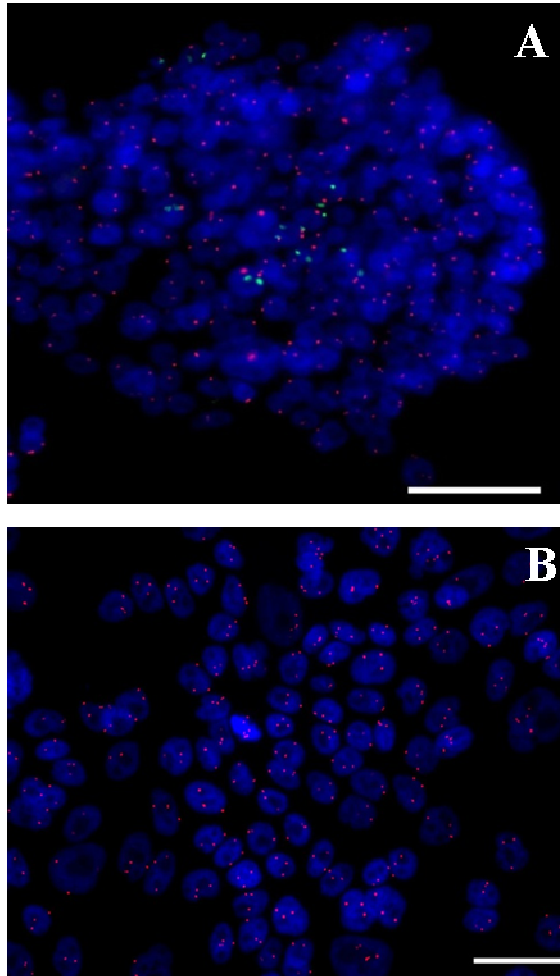


Figure 6: FISH analysis on cultured TEpC (A) and Calu-3 (B) cell lines. Sex X and Y chromosomes are visualized by red and green fluorescence, respectively. Nuclei are recognized by the blue fluorescence of DAPI. Scale bars:50 μ m

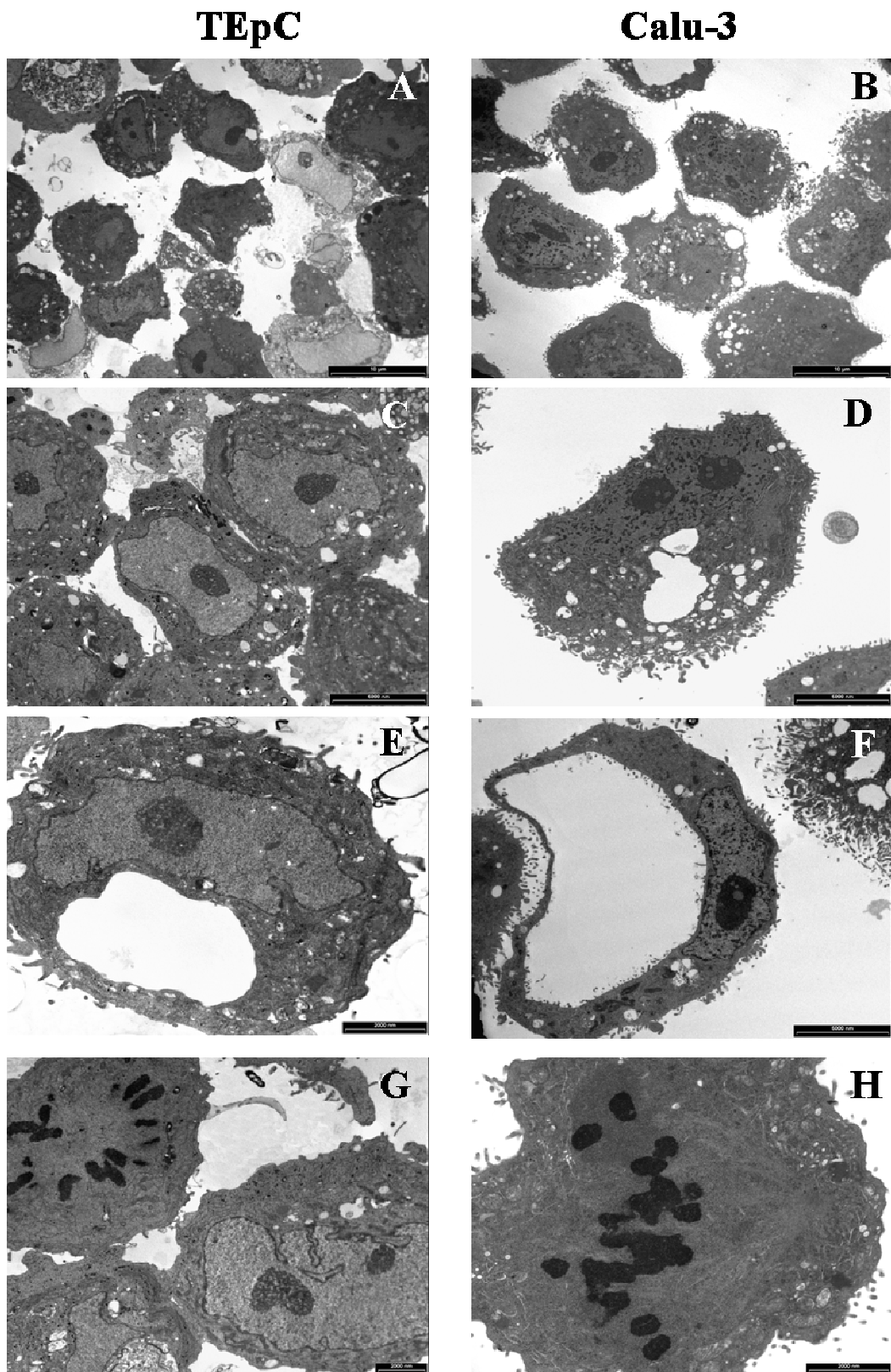
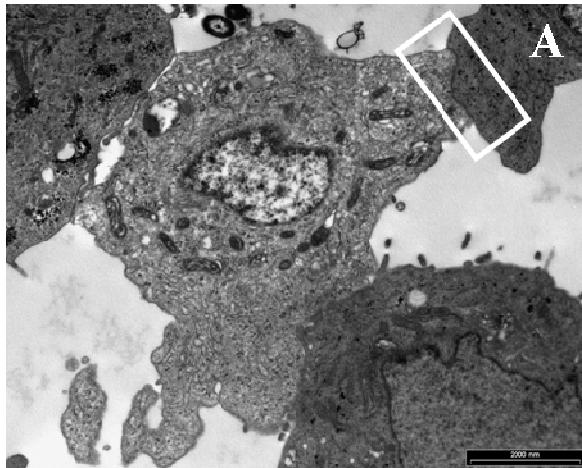


Figure 7: Ultrastructural analysis of TEpC and Calu-3. TEM images show similar subcellular characteristics, as intracytoplasmic vacuoles and nuclear chromatin condensation (A-D). Panels E and F show typical adenocarcinoma “signet ring” feature in both TEpC and Calu-3 samples. Mitotic figures in TEpC (G) and Calu-3(H) are illustrated.

TEpC



Calu-3

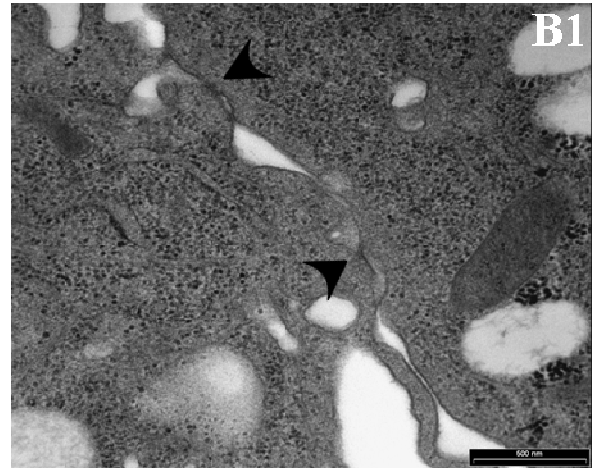
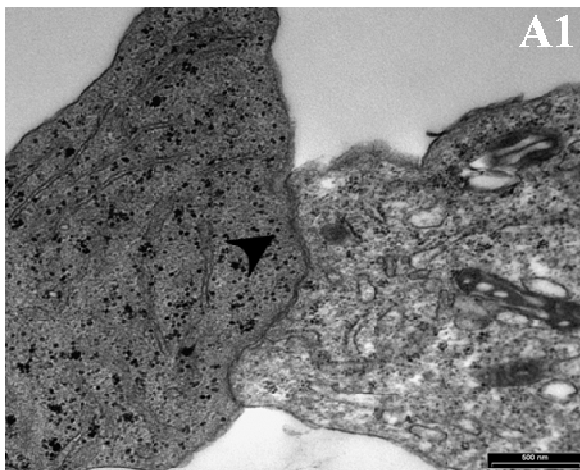
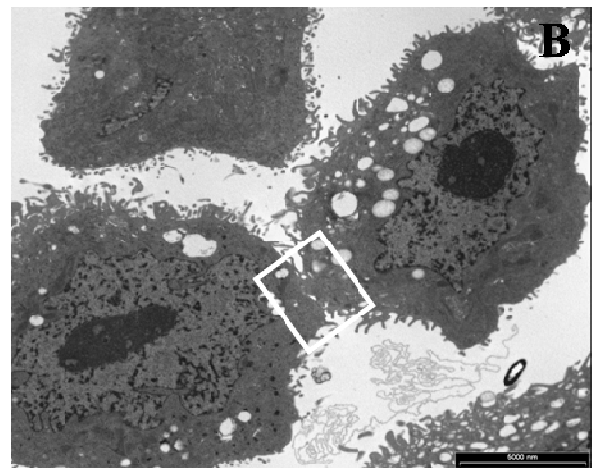


Figure 8: Ultrastructural analysis of TEpC and Calu-3. A and B TEM images show the presence of preserved intercellular adherence junctions in TEpC and Calu-3, respectively. Adherence junctions are shown at higher magnification in A1 and B1 (arrowheads).

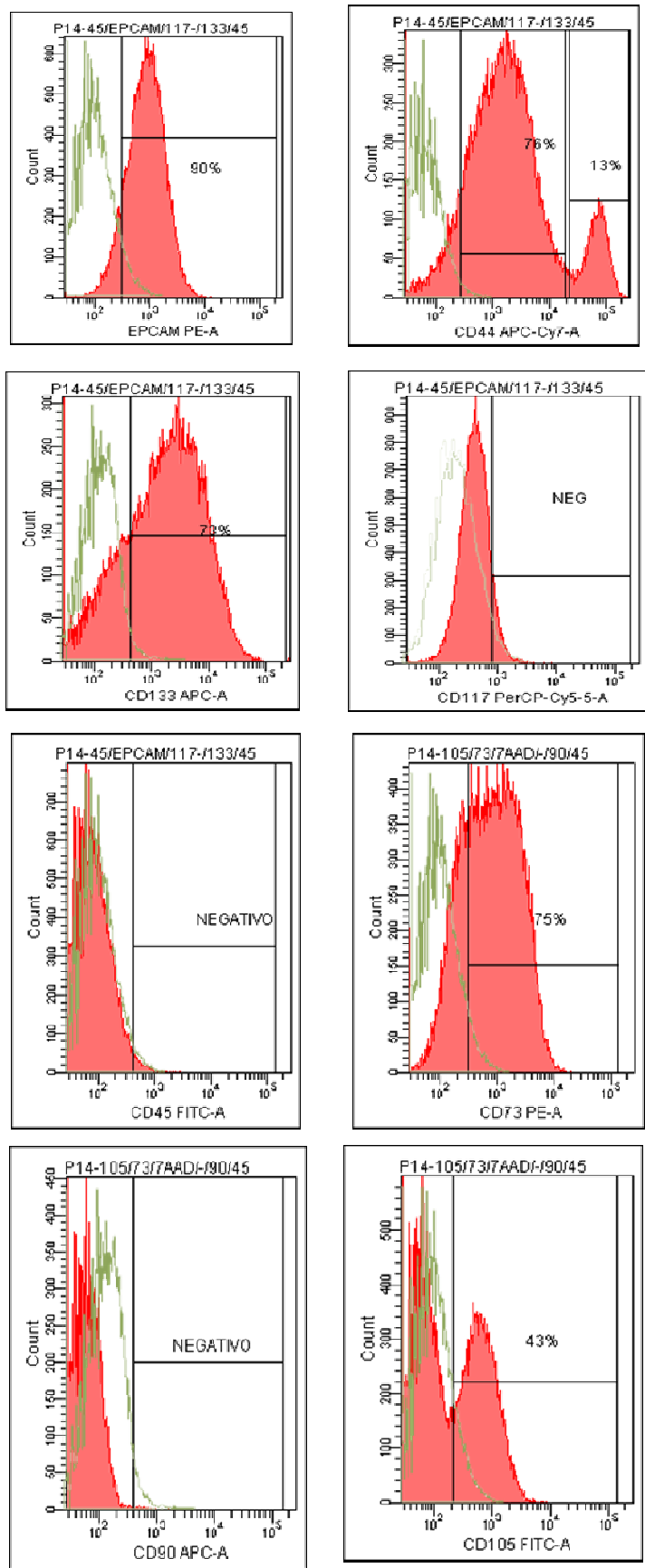


Figure 9: FACS analysis on TEpC at passage 14 of *in vitro* amplification

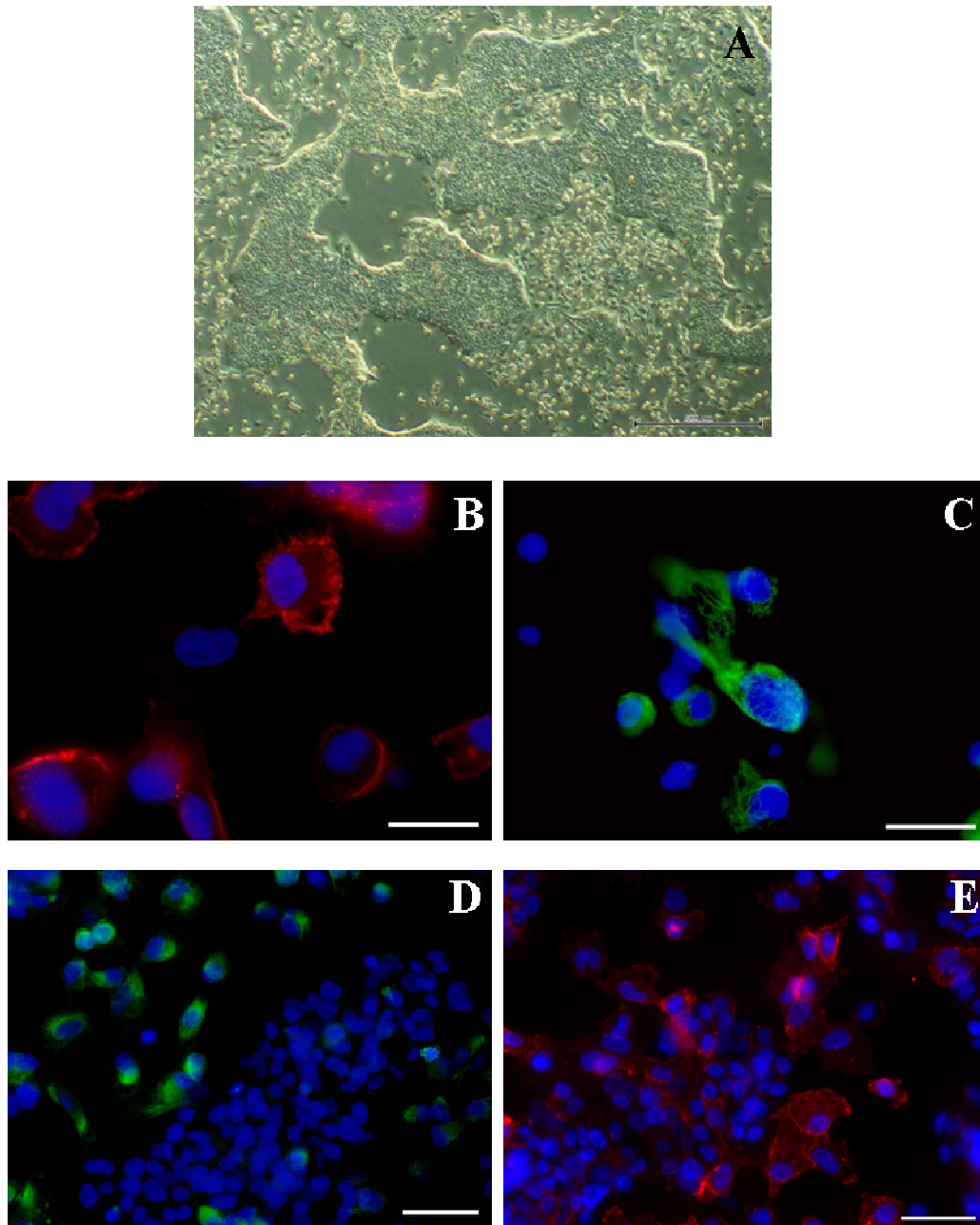


Figure 10: Phase contrast image of TEpC population at p14 (A). Immunocytochemical characterization of these cells by the detection of epithelial markers E-Cad (B) and panCK (C) shown in red and green fluorescence, respectively. The mesenchymal markers Vimentin (D, green fluorescence) and CD44 (E, red fluorescence) were also detected. Scale bars A: 500 μm , B and C :30 μm ; D and E :50 μm

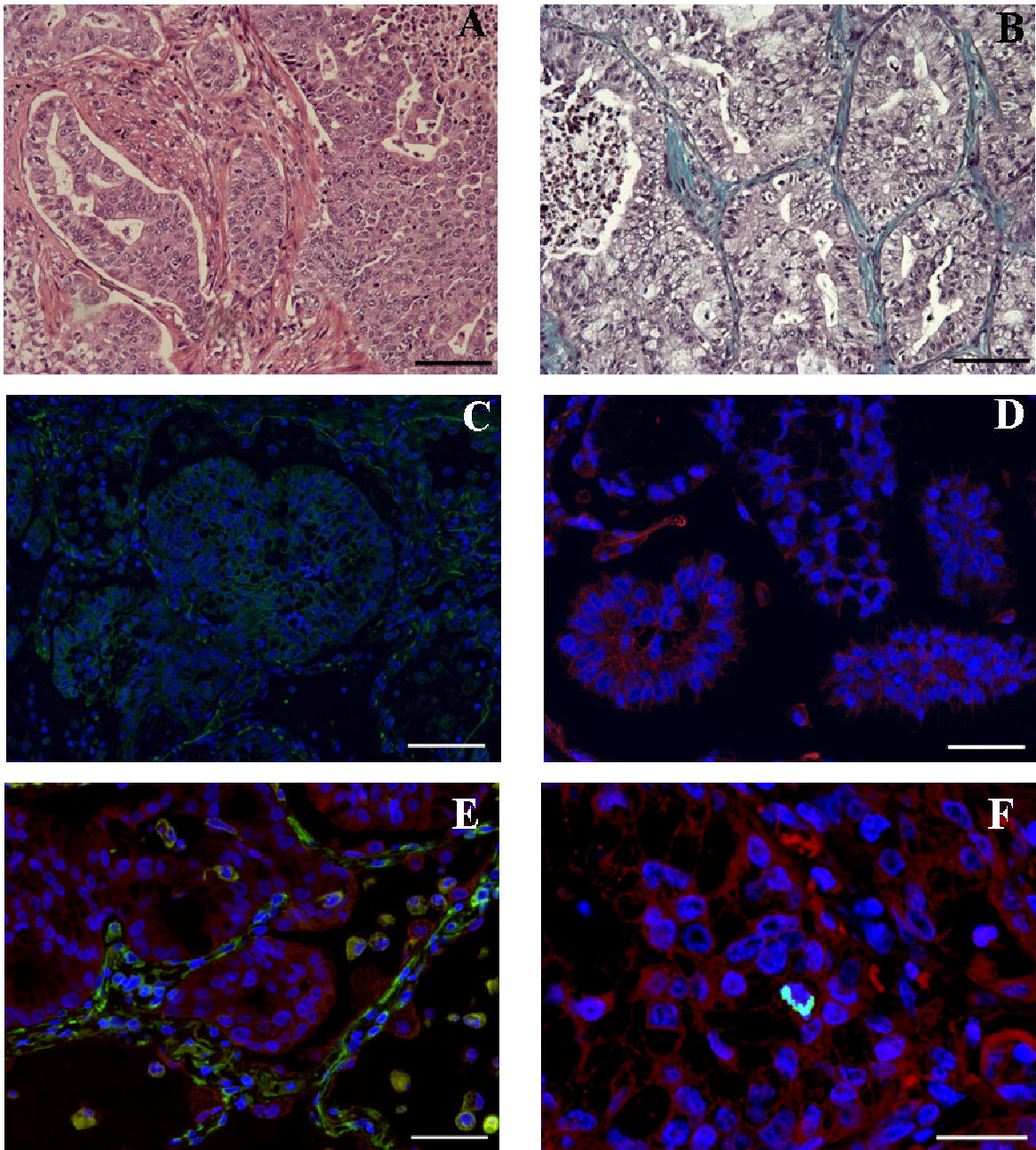
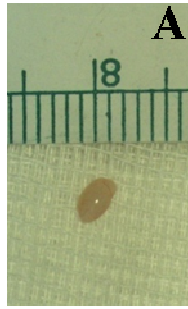


Figure 11: Human primary lung adenocarcinoma. Hystological preparations of lung cancer tissue stained by H&E (A) and Masson's Trichrome (B). Epithelial glands are positive for E-Cad (C, green fluorescence) and CD44 (D, red fluorescence). In panel E, double immunostaining for panCK (red fluorescence) and Vim (green fluorescence) illustrates neoplastic glands surrounded by stromal cells. Panel F: mitotic divisions in panCK positive (red fluorescence) cells are shown by the green fluorescence of phosphohistone H3. Scale bars A-C :100 μ m, D-E :50 μ m; F :30 μ m

TEpC Xenograft



Calu-3 Xenograft

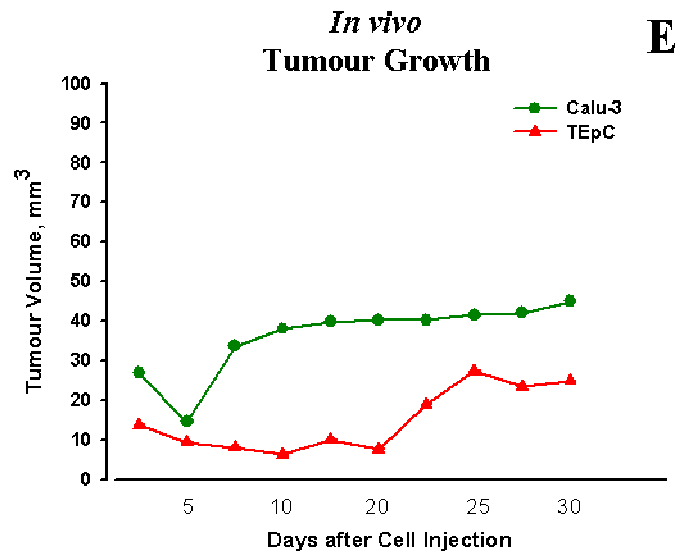
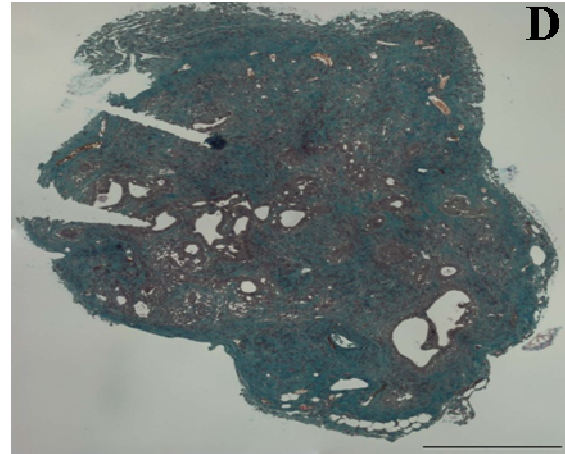
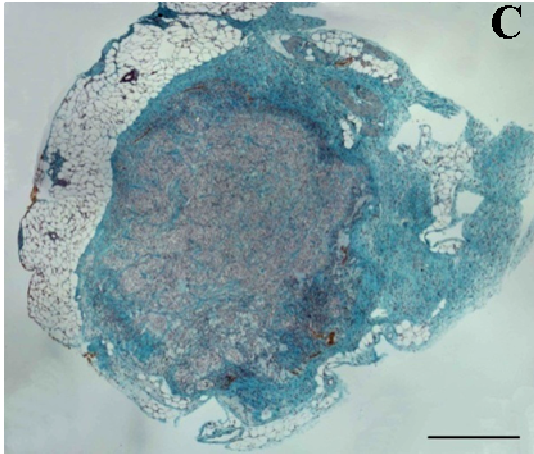
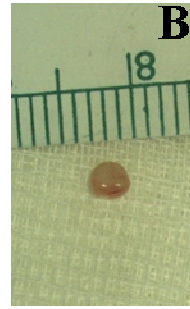


Figure 12: Macrophotographs of nodules excised from TEpC (A) and Calu-3 (B) injected mice. Hystological analysis was performed on Masson's trichrome staining of sections from TEpC (C) and Calu-3 (D) tumour xenografts. The line graph highlights the *in vivo* tumour growth in the two experimental groups. Scale bars :500 μ m.

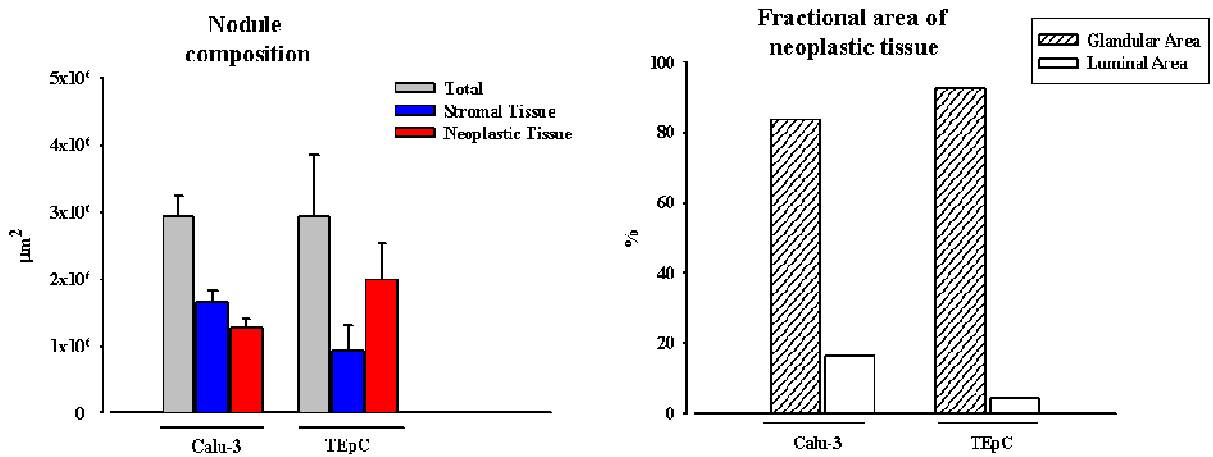
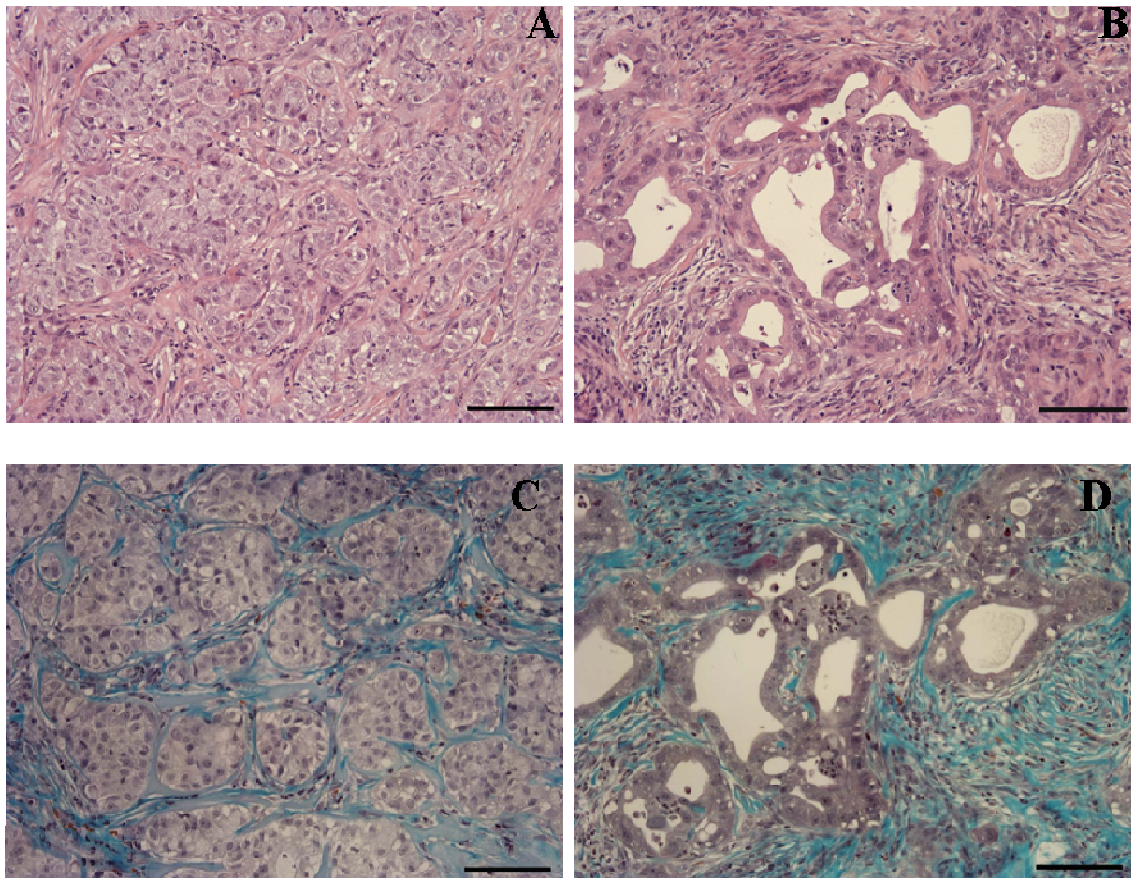


Figure 13: Hystological analysis of tumour xenografts of TEpC and Calu-3 by H&E (A and B) and Masson's Trichrome (C and D). Morphometric quantification of nodule composition and fractional area of neoplastic structures are reported in graph E and F, respectively. Scale bars :100 μm

TEpC Xenograft

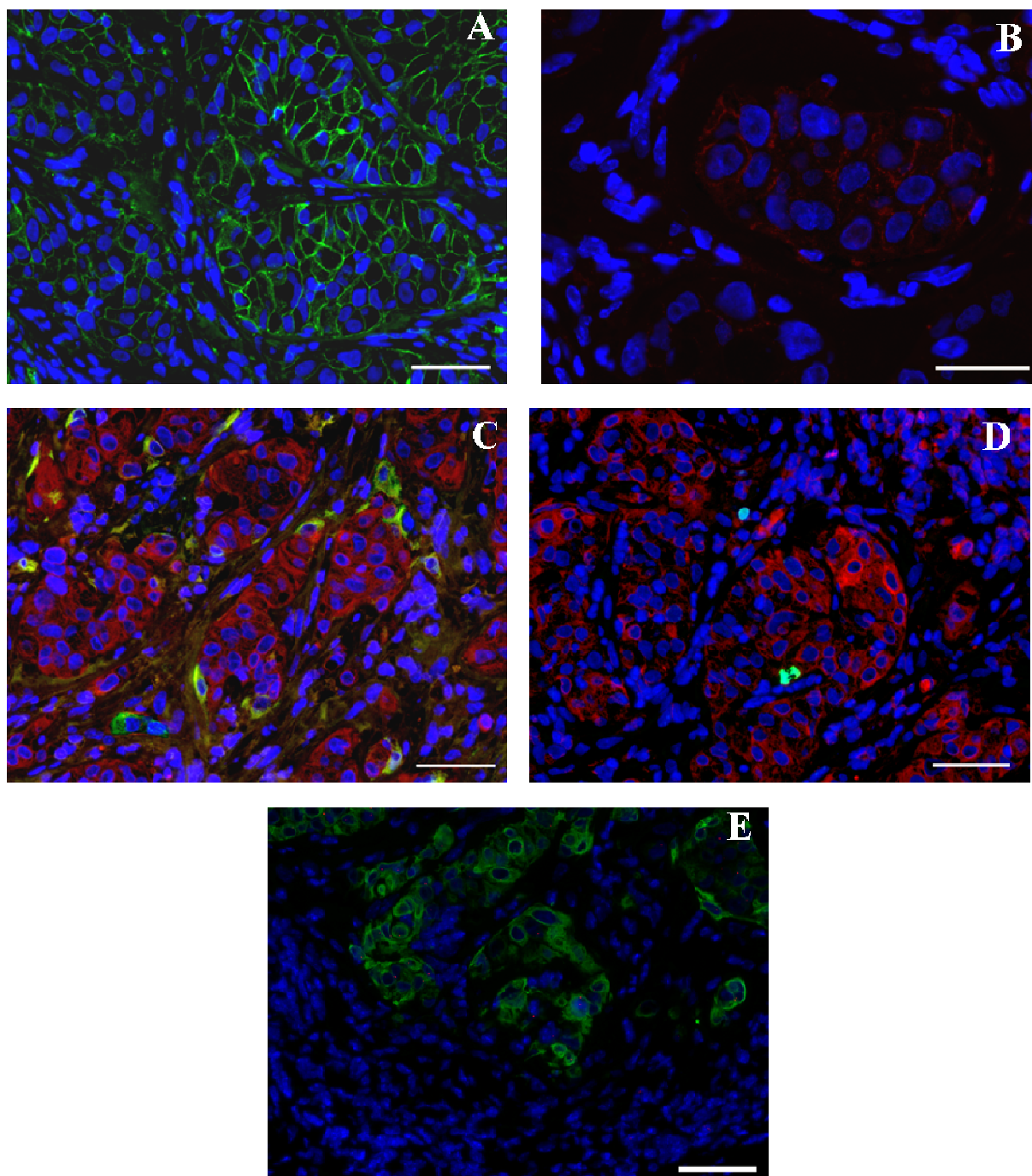


Figure 14: Sections of TEpC nodule. Immunohistochemical detection of E-Cadherin (A, green) and CD44 (B, red). Microphotograph in C shows Pan-cytokeratin (red fluorescence) and Vimentin (green fluorescence) expression. Mitotic divisions in panCK positive (red fluorescence) cells are shown by the green fluorescence of phosphohistone-H3 (D). Panel E shows the localization of Human sexual chromosomes XY in the tumour cells stained for panCK (green fluorescence). Nuclei are recognized by the blue fluorescence of DAPI. Scale bars: 50 μ m

Calu-3 Xenograft

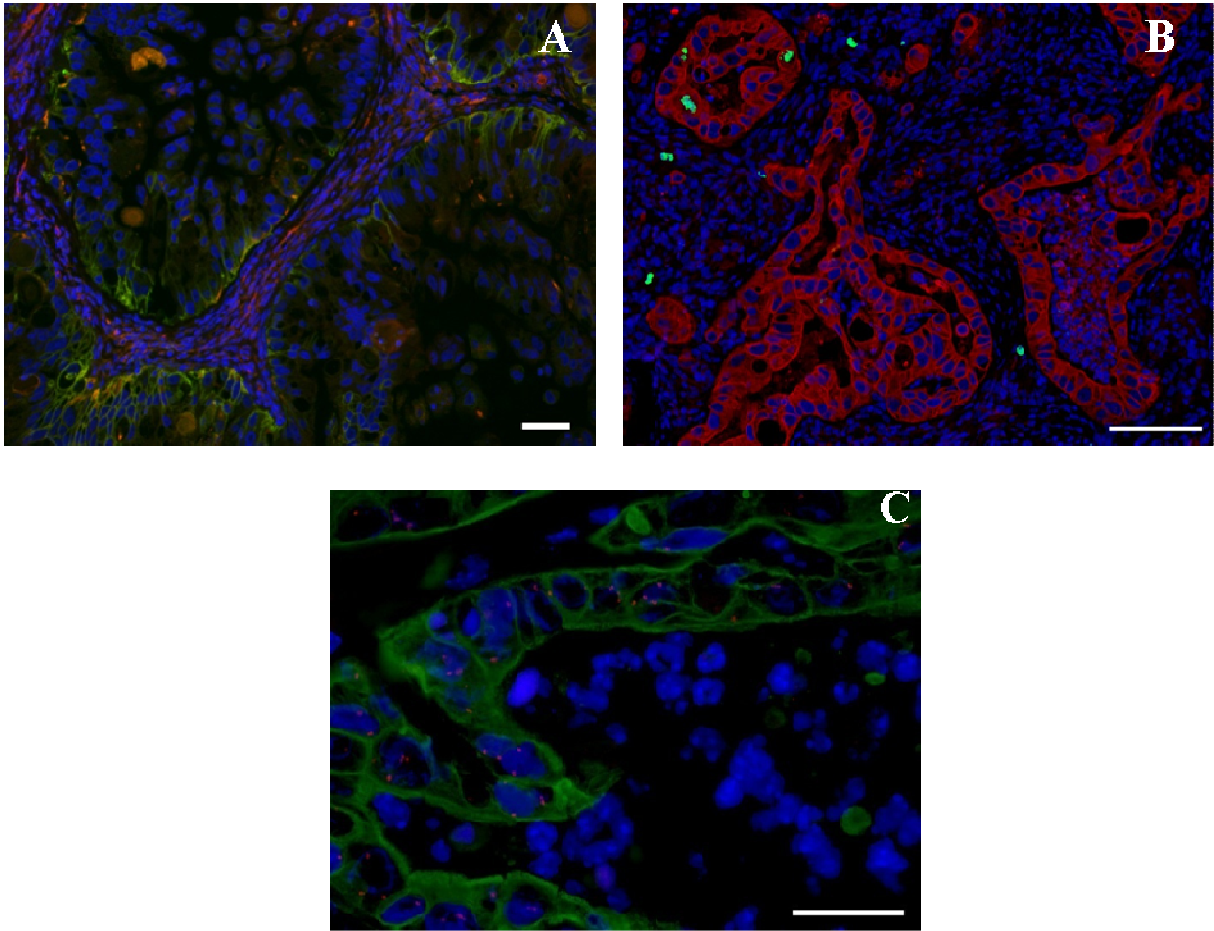


Figure 15: Sections of Calu-3 nodule. Immunohistochemical detection of Vimentin and CD44 showed in green and red fluorescence, respectively (A). Mitotic cell positive for pH3 (green fluorescence) and panCK (red fluorescence) are detected in panel B. Panel C: FISH analysis of human X chromosome (red fluorescence) associated to panCK staining (green fluorescence) to confirm the human tumoral origin of xenografts. Nuclei are recognized by the blue fluorescence of DAPI. Scale bars A and B: 100 μm ; C: 50 μm

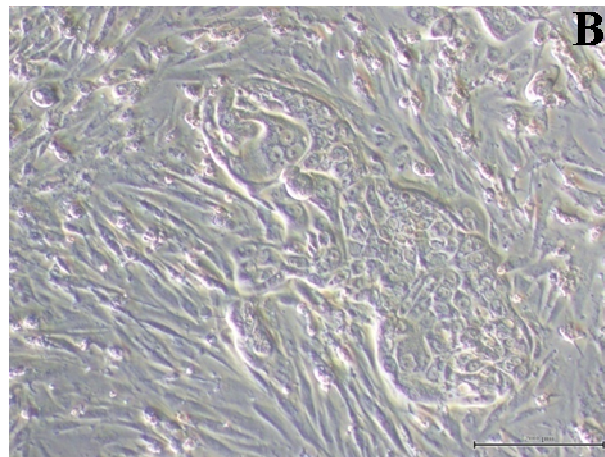
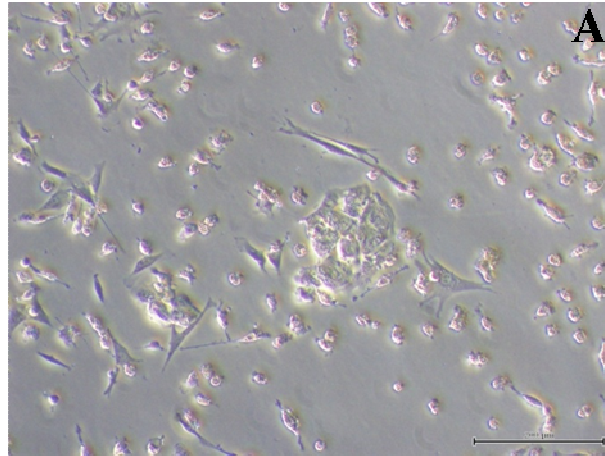


Figure 16: Phase contrast images of TEpC (A) and Calu-3 (B) re-expanded after their isolation from excised tumour xenografts. Scale bars 200 μm

References

-
- ¹ Jemal A, Bray F, Center MM, et al. *Global cancer statistics*. CA Cancer J Clin 2011;61:69-90.
- ² Malvezzi M, Bertuccio P, Levi F, et al. *European cancer mortality predictions for the year 2012*. Ann Oncol 2012; 23: 1044–1052.
- ³ De Matteis S, Consonni D, Lubin JH, Tucker M, Peters S, Vermeulen RCh, Kromhout H, Bertazzi PA, Caporaso NE, Pesatori AC, Wacholder S, Landi MT. *Impact of occupational carcinogens on lung cancer risk in a general population*. Int J Epidemiol. 2012 Jun;41(3):711-21. doi: 10.1093/ije/dys042. Epub 2012 Mar 31.
- ⁴ Brennan P, Hainaut P, Boffetta P. *Genetics of lung-cancer susceptibility*. Lancet Oncol.12(4):399-408;2011
- ⁵ Morgan R. Davidson, Adi F. Gazdar, Belinda E. Clarke. *The pivotal role of pathology in the management of lung cancer*. Review J Thorac Dis 2013;5(S5):S463-S478. doi: 10.3978/j.issn.2072-1439.2013.08.43.
- ⁶ Johnson BE, Grayson J, Makuch RW, et al.: *Ten-year survival of patients with small-cell lung cancer treated with combination chemotherapy with or without irradiation*. J Clin Oncol 8 (3): 396-401, 1990.
- ⁷ Lassen U, Osterlind K, Hansen M, et al. *Long-term survival in small-cell lung cancer: posttreatment characteristics in patients surviving 5 to 18+ years--an analysis of 1,714 consecutive patients*. J Clin Oncol 13 (5): 1215-20, 1995.
- ⁸ Wendy A. Cooper, David C. L. Lam, Sandra A. O'Toole, John D. Minna *Molecular biology of lung cancer* Review J Thorac Dis 2013;5(S5):S479-S490. doi: 10.3978/j.issn.2072-1439.2013.08.03.
- ⁹ Kosaka T, Yatabe Y, Endoh H, et al. *Mutations of the epidermal growth factor receptor gene in lung cancer: biological and clinical implications*. Cancer Res 2004;64:8919-23.
- ¹⁰ Shigematsu H, Lin L, Takahashi T, et al. *Clinical and biological features associated with epidermal growth factor receptor gene mutations in lung cancers*. J Natl Cancer Inst 2005;97:339-46.
- ¹¹ Koivunen JP, Mermel C, Zejnullahu K, et al. *EML4-ALK fusion gene and efficacy of an ALK kinase inhibitor in lung cancer*. Clin Cancer Res 2008;14:4275-83.
- ¹² Bean J, Brennan C, Shih JY, et al. *MET amplification occurs with or without T790M mutations in EGFR mutant lung tumors with acquired resistance to gefitinib or erlotinib*. Proc Natl Acad Sci USA 2007;104:20932-7.
- ¹³ McCulloch EA, Till JE. *Perspectives on the properties of stem cells*. Nat Med.11(10):1026-8 2005.
- ¹⁴ D. Leanne Jones and Amy J. Wager. *No place like home: anatomy and function of the stem cell niche*. Nat Rev Mol Cell Biol. 2008 Jan;9(1):11-21.

-
- ¹⁵ Kajstura J, Rota M, Hall SR, Hosoda T, D'Amario D, Sanada F, Zheng H, Ogórek B, Rondon-Clavo C, Ferreira-Martins J, Matsuda A, Arranto C, Goichberg P, Giordano G, Haley KJ, Bardelli S, Rayatzadeh H, Liu X, Quaini F, Liao R, Leri A, Perrella MA, Loscalzo J, Anversa P. *Evidence for human lung stem cells*. N Engl J Med. 2011 May 12;364(19):1795-806. doi: 10.1056/NEJMoa1101324.
- ¹⁶ Darrell N. Kotton & Alan Fine. *Lung stem cells*. Review Cell Tissue Res (2008) 331:145–156.
- ¹⁷ Giangreco A, Groot KR, Janes SM. *Lung cancer and lung stem cells: strange bedfellows?* Am J Respir Crit Care Med., 2007 Mar 15;175(6):547-53. Epub 2006 Dec 7.
- ¹⁸ Kim CF, Jackson EL, Woolfenden AE, Lawrence S, Babar I, Vogel S, Crowley D, Bronson RT, Jacks T. *Identification of bronchioalveolar stem cells in normal lung and lung cancer*. Cell 121(6):823-35; 2005.
- ¹⁹ Al-Hajj, et al., *Prospective identification of tumorigenic breast cancer cells*. Proc Natl Acad Sci USA 100: 3983-3988, 2003.
- ²⁰ Lapidot T., et al., *A cell initiating human acute myeloid leukaemia after transplantation into SCID mice*. Nature 367: 645-648, 1994.
- ²¹ Singh S.K., et al., *Identification of human brain tumour initiating cells*. Nature 432: 396-401, 2004.
- ²² Fábrián A, Barok M, Vereb G, Szölloši J. *Die hard: are cancer stem cells the Bruce Willises of tumor biology?* Cytometry A.75(1):67-74; 2009.
- ²³ Sales KM, Winslet MC, Seifalian AM. *Stem cells and cancer: an overview*. Stem Cell Rev. 3(4):249-55; 2007.
- ²⁴ Guarino M., Rubino B., Ballabio G. *The role of epithelial-mesenchymal transition in cancer pathology*. Pathology. 2007 Jun;39(3):305-18.
- ²⁵ Thiery JP, Acloque H, Huang RY, Nieto MA. *Epithelial-mesenchymal transitions in development and disease*. Cell. 2009 Nov 25;139(5):871-90. doi: 10.1016/j.cell.2009.11.007. Review.
- ²⁶ Willipinski-Stapelfeldt B, Riethdorf S, Assmann V et al. *Changes in cytoskeletal protein composition indicative of an epithelial-mesenchymal transition in human micrometastatic and primary breast carcinoma cells*.2005 Clin Cancer Res 11(22):8006–8014.
- ²⁷ Buck E, Eyzaguirre A, Barr S et al. *Loss of homotypic cell adhesion by epithelial-mesenchymal transition or mutation limits sensitivity to epidermal growth factor receptor inhibition*. 2007 Mol Cancer Ther 6(2):532–541.
- ²⁸ Umbas R, Schalken JA, Aalders TW et al. *Expression of the cellular adhesion molecule E-cadherin is reduced or absent in high-grade prostate cancer*. 1992 Cancer Res 52(18):5104–5109.
- ²⁹ Perl AK, Wilgenbus P, Dahl U et al. *A causal role for Ecadherin in the transition from adenoma to carcinoma*. 1998 Nature 392(6672):190–193

-
- ³⁰ Mani SA, Guo W, Liao MJ, Eaton EN, Ayyanan A, Zhou AY, Brooks M, Reinhard F, Zhang CC, Shipitsin M, Campbell LL, Polyak K, Brisken C, Yang J, Weinberg RA. *The epithelial-mesenchymal transition generates cells with properties of stem cells*. Cell. 2008 May 16;133(4):704-15. doi: 10.1016/j.cell.2008.03.027.
- ³¹ Suda K, Tomizawa K, Fujii M, Murakami H, Osada H, Maehara Y, Yatabe Y, Sekido Y, Mitsudomi T. *Epithelial to mesenchymal transition in an epidermal growth factor receptor-mutant lung cancer cell line with acquired resistance to erlotinib*. J Thorac Oncol. 2011 Jul;6(7):1152-61. doi: 10.1097/JTO.0b013e318216ee52.
- ³² Nurwidya F, Takahashi F, Murakami A, Takahashi K. *Epithelial mesenchymal transition in drug resistance and metastasis of lung cancer*. Cancer Res Treat. 2012 Sep;44(3):151-6. doi: 10.4143/crt.2012.44.3.151.
- ³³ Cavazzoni A, Alfieri RR, Cretella D, Saccani F, Ampollini L, Galetti M, Quaini F, Graiani G, Madeddu D, Mozzoni P, Galvani E, La Monica S, Bonelli M, Fumarola C, Mutti A, Carbognani P, Tiseo M, Barocelli E, Petronini PG, Ardizzoni A. *Combined use of anti-ErbB monoclonal antibodies and erlotinib enhances antibody-dependent cellular cytotoxicity of wild-type erlotinib-sensitive NSCLC cell lines*. Mol Cancer. 2012 Dec 12;11:91. doi: 10.1186/1476-4598-11-91.
- ³⁴ T. Friess, W. Scheuer and M. Hasmann. *Erlotinib Antitumor Activity in Non-small Cell Lung Cancer Models is Independent of HER1 and HER2 Overexpression*. 2006 Anticancer Research 26: 3505-3512.